



**OTC-26032-MS**

## **Novel Anchoring Solutions for FLNG - Opportunities Driven by Scale**

C.D. O'Loughlin, D.J. White, and S.A. Stanier, Univ. of W. Australia (UWA)

Copyright 2015, Offshore Technology Conference

This paper was prepared for presentation at the Offshore Technology Conference held in Houston, Texas, USA, 4–7 May 2015.

This paper was selected for presentation by an OTC program committee following review of information contained in an abstract submitted by the author(s). Contents of the paper have not been reviewed by the Offshore Technology Conference and are subject to correction by the author(s). The material does not necessarily reflect any position of the Offshore Technology Conference, its officers, or members. Electronic reproduction, distribution, or storage of any part of this paper without the written consent of the Offshore Technology Conference is prohibited. Permission to reproduce in print is restricted to an abstract of not more than 300 words; illustrations may not be copied. The abstract must contain conspicuous acknowledgment of OTC copyright.

---

### **Abstract**

FLNG facilities present a more onerous anchoring requirement than existing floating structures. Optimisation of the anchoring technology through improved design or through novel anchor types offers potential cost and risk benefits. These benefits may also be applicable to smaller moorings for MODUs and FPSOs. This paper uses concept-level design calculations of anchor capacity to compare different anchor technologies in the context of FLNG and MODU/FPSO applications. Also, new observations from physical modelling of chain-soil interaction are presented. Opportunities are identified for significant cost and schedule savings by adopting the alternative plate anchor technologies that are either suction or dynamically installed. Considering fabrication alone, the estimated costs are reduced by 70% for FLNG and 80% for MODUs relative to the conventional suction caisson option. When installation vessel costs are considered, the absolute cost saving could be far higher than from fabrication alone because installation could be from an anchor-handling vessel rather than a construction barge with a heavy lift crane. Torpedo anchors have also been considered, but are less attractive. Centrifuge model data and calculations of the shape and capacity of the embedded anchor chain suggest that there may be over-looked capacity from the mooring chain both on and within the seabed. At the same time, upscaling of embedded plates to the scale required for FLNG applications increases the amount of chain slack that would be released into the mooring during in service loading, and this effect requires consideration in the overall mooring system design. Research and development activities aligned with the opportunities for reduced cost and risk in anchoring design are set out.

### **Introduction**

The development of large FLNG vessels on the scale of Shell's 492 m-long Prelude facility creates an onerous requirement for anchoring, particularly when deployed in cyclone-prone regions such as offshore Australia's North West coast. The Prelude field is in relatively shallow water, and will be anchored by 16 driven piles, 5.5m in diameter and 65 m long (Shell 2014).

The larger FLNG anchor loads are a step-out in scale relative to typical floating facilities, so there is the possibility that the optimal anchoring arrangement will differ from current practice. Also, novel anchor technologies have recently emerged and offer potential benefits relative to conventional solutions.

This paper explores the potential use of novel technologies to optimise the anchoring of FLNG facilities. Also, the application of these new technologies in less onerous cases is explored, including

MODU and FPSO moorings, and potentially temporary anchoring of FLNG vessels where lower design loads may apply. The increasing use of subsea wells including for FLNG projects raises the requirement for frequent visits by MODUs for workovers. Recently-developed anchor technologies may permit more rapid and cost-effective deployment of anchoring, reducing non-productive drilling unit time.

Concept-level design calculations of anchor capacity are used to compare different technologies in the context of a potential deep water FLNG design scenario, using typical mooring line loads and soil conditions found in deepwater frontier regions. Based on the anchor sizes derived from the capacity calculations, the anchor types are compared more broadly, including the risks, costs and schedule for installation.

A summary of the existing research and industry experience associated with each anchor technology is also provided, focusing on the maturity of each anchor type and the steps that will be required to advance the less mature technologies through to deployment. Three central issues are tackled:

- The feasibility of the step-out in scale from existing experience required for future FLNG applications – illustrated via concept-level calculations of anchor sizing.
- An analysis of the gaps, uncertainties and barriers associated with the application of innovative anchor technologies – for example, in relation to the maturity of design methods and the verification/qualification process.
- An analysis of the prize associated with innovative anchor technologies – for example, in relation to vessel requirements, installation duration and cost.

In addition, the influence of the embedded chain on the overall anchor performance is considered by example analyses. Results from geotechnical centrifuge testing are used to illustrate potential improvements in the treatment of chain-seabed interaction.

The paper ends by summarising the most promising opportunities for improved anchoring solutions for FLNG and smaller vessels. The activities required to overcome the remaining barriers to deployment are also outlined.

## Anchor types

The paper focuses on four anchor types that range from the well-established standard solution for deepwater soft soils (suction caisson), to novel technologies that offer promise based on small scale trials but which have not yet been qualified for project use (the DEPLA). The four anchor types are:

1. Suction caisson
2. Suction-embedded plate anchor (SEPLA)
3. Dynamically-embedded torpedo anchor
4. Dynamically-embedded plate anchor (DEPLA)

The anchors are illustrated in [Figure 1](#) and the key dimensions are introduced in [Figure 2](#). Further information regarding their installation and loading modes are given below. An exhaustive literature review on the design and performance of these anchors cannot be provided in a single paper, but the relevant information can be found in [Randolph and Gourvenec \(2011\)](#) and in the references provided for each anchor type in the following sections.

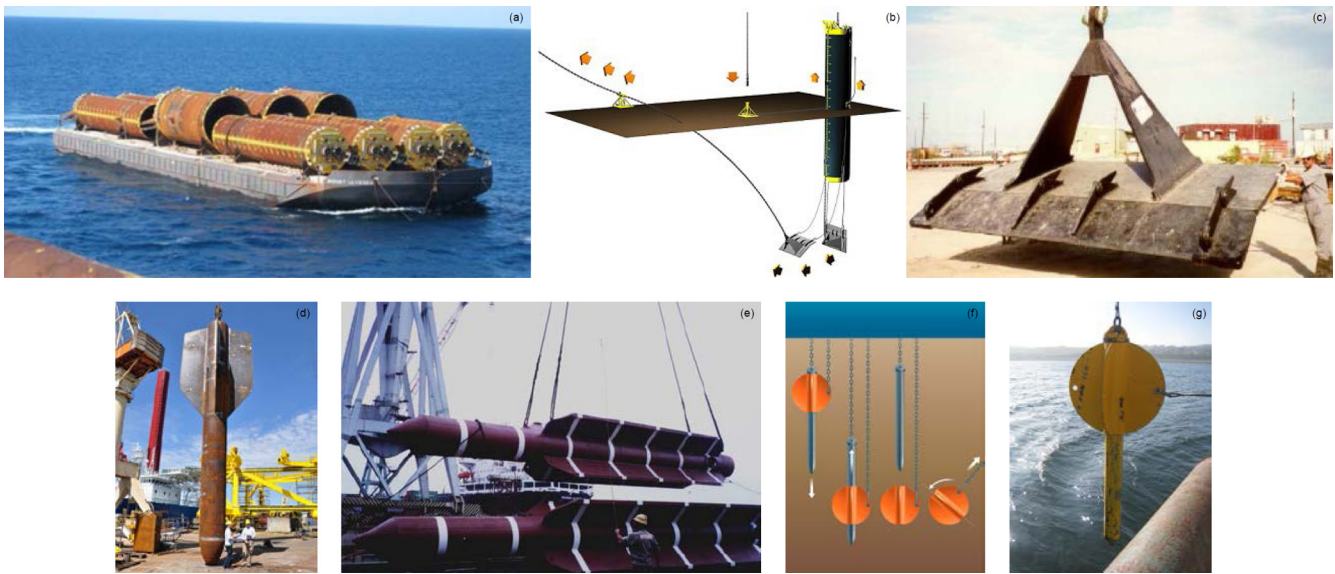


Figure 1—Example of each anchor type: (a) suction caisson, (b, c) SEPLA, (d, e) torpedo anchor, (f, g) DEPLA.

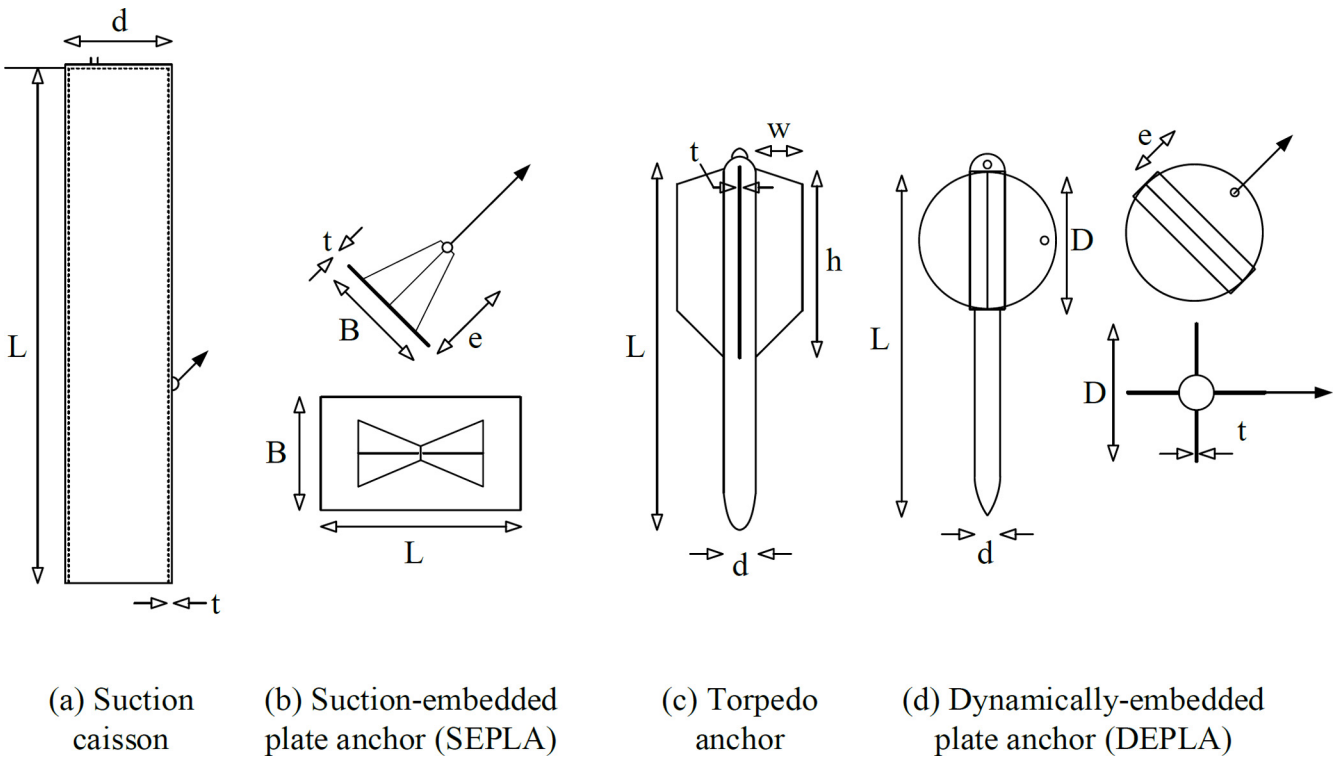


Figure 2—Key dimensions of each anchor type.

## Suction caisson

A suction caisson is a thin-walled steel cylinder, closed at the top, with a typical range of aspect ratios, length to diameter  $L/d = 4 - 10$ . They have overall lengths of up to  $\sim 40$  m and dry masses of up to  $\sim 250$  tonnes. Installation is initially by lowering until the full caisson self-weight is applied to the seabed, followed by pumping water from the inside of the caisson to create a pressure difference ('suction') that creates further penetration until the top cap is flush with the soil surface. Load is transferred to the caisson through a padeye located part way down the caisson. The capacity of the caisson is derived from both

passive pressure and sliding resistance against the caisson wall. Failure may involve rotation of the caisson, vertical pullout or a combination of these mechanisms, depending on the mooring line inclination at the padeye, which is affected by the shape of the inverse catenary taken by the mooring line in the soil.

### Suction-embedded plate anchor

A suction-embedded plate anchor (SEPLA) uses a suction caisson to install a plate anchor that is fixed into a slot at its base. The caisson is installed in the usual manner, and then retrieved for re-use in the next installation leaving the plate anchor buried vertically in the seabed (see [Figure 1b](#)). The plate anchor is typically rectangular with a plate aspect ratio, height to width,  $B/L = 1.5 - 2$ , and a padeye that is offset from the plate on a shank. The caisson length is dictated by the target embedment depth. Previous applications have used caissons with lengths of typically 24 m and a typical caisson aspect ratio,  $L/d = 5$ .

Load is applied to the plate by a chain attached to the pad-eye. As the load is increased the plate anchor rotates to become perpendicular to the mooring line, in order to mobilise the full capacity. This process is known as ‘keying’ of the anchor. During this rotation the embedment of the anchor may reduce, which will have some effect on anchor capacity, although this may be minimised by ensuring that the padeye is offset from the anchor plate by at least half a plate height. However, the keying process also causes chain slack in the mooring line, which may alter the static and dynamic response of the mooring. SEPLA capacity is due to passive soil pressure on the face of the plate, with small additional components from the shank. Further information can be found in Gaudin et al. ([2010, 2015](#)), Cassidy et al. ([2012](#)) and Yang et al. ([2012](#)).

### Dynamically-embedded torpedo anchor

Dynamically-embedded torpedo anchors are long cylindrical anchors with a rounded or conical front tip and fins towards the rear of the cylindrical shaft. They are installed by allowing the anchor to freefall from a designated height above the seabed, such that the anchor impacts the seafloor at close to the terminal velocity and self-buries in the seabed. Torpedo anchors typically have an aspect ratio, length to diameter,  $L/d = 10 - 20$  and a dry mass of up to 120 tonnes. They are typically released from up to 100 m above the seafloor and impact the seabed with velocities of up to 30 m/s, achieving anchor tip embedments of up to three times their overall length. Anchor holding capacity is mainly generated from the frictional resistance that develops along the anchor-soil interface, and potentially also through passive pressure if the mooring line inclination and load causes the anchor to rotate (Richardson et al. ([2009](#)), O’Loughlin et al. ([2013](#))).

### Dynamically-embedded plate anchor

The dynamically embedded plate anchor (DEPLA) comprises a removable central shaft or ‘follower’ and a set of four flukes arranged on a cylindrical sleeve and connected to the follower with a shear pin. The DEPLA is installed in a similar manner to other dynamically installed anchors, by releasing the anchor from a height above the seafloor. The height is chosen such that the anchor will impact the seabed at a velocity approaching its terminal velocity and subsequently self-bury in the seafloor. After the DEPLA has come to rest in the seabed, the follower retriever line is tensioned. This causes the shear pin to part (if not already broken during impact) allowing the follower to be retrieved and reused for the next installation, whilst leaving the anchor flukes vertically embedded in the seabed. These embedded anchor flukes constitute the load bearing element as a plate anchor. When sufficient load develops in the mooring line, the plate rotates to an orientation that is approximately perpendicular to the direction of loading at the pad-eye, allowing the full bearing resistance of the plate to be mobilised. The DEPLA and its installation and keying processes are summarised in [Figure 1f](#).

### Performance data and technology maturity of each anchor type

The suction caisson is the most mature of the candidate anchor types, as it is already used extensively for MODU, spar platform and FPSO permanent mooring applications. Available performance data include

installation records from centrifuge and field studies and centrifuge capacity data. An overview of these performance data spanning over two decades is provided in Andersen et al. (2005).

The torpedo anchor arguably follows in terms of technology maturity as it has been used extensively for both temporary and permanent facilities offshore Brazil (Brandao et al. 2006, Henriques et al. 2010). It has also been used for temporary facilities in the Gulf of Mexico (Zimmerman et al. 2009), although the design used in the Gulf of Mexico is quite different to that used offshore Brazil. The majority of performance data are from centrifuge studies (O'Loughlin et al. 2004, 2009, 2013; Richardson et al. 2006, 2009; Gaudin et al. 2013; Hossain et al. 2015) although a growing body of field experience is becoming available (Zimmerman et al. 2009, O'Beirne et al. 2015).

The first field trials on suction embedded plate anchors took place between 1999 and 2001 (Wilde et al. 2001) and since then they have been used mainly for temporary moorings, although they have also been considered as permanent moorings for mobile facilities (Wong et al. 2012). To the authors' knowledge there are no reported instances of their use with permanent facilities. The first available performance data was from field trials (Wilde et al. 2001) and since then performance data have been gathered from centrifuge studies that mainly focused on keying behaviour in an attempt to optimize the plate geometry, particularly the location of the padeye relative to the plate (O'Loughlin et al. 2006; Song et al. 2009; Wang et al. 2011; Gaudin et al. 2006, 2010, 2015; Cassidy et al. 2012, Yang et al. 2012, Wong et al. 2012; Tian et al. 2014).

The least mature anchor technology is the dynamically-embedded plate anchor, which has been proven through centrifuge studies and quite extensively in the field, albeit at quarter scale (O'Loughlin et al. 2013, 2014, 2015; Blake and O'Loughlin 2012, 2015; Blake et al. 2015).

Table 1 provides a very brief overview of the maturity of each anchor technology, together with the design methods and codes relevant for each anchor type.

**Table 1—Technology maturity for each anchor option**

Maturity aspect	Anchor type			
	Suction caisson	SEPLA	Torpedo anchor	DEPLA
Invented	1980s	1997	~1995	2004
Experience	Base case anchor system for soft clay and large FPSOs and spars.	Field trials: 1999–2001. MODUs in GoM: 2000. MODUs in W. Africa: 2003. One published use for permanent (10 year) mooring.	Field trials during late 1990s by Petrobras. Used widely offshore Brazil for MODUs and FPUs. OMNI-Max variant used in GoM for temporary moorings.	Invented by UWA. Installation trials in 2005 at small scale offshore (Timor Sea). Installation and capacity trials at centrifuge scale and at reduced field scale (1/4) in lake (Ireland) and nearshore (Scotland) 2009–13.
Design methods	Installation: design methods are reliable and mature, uncertainties may relate to particular soil types (e.g. carbonates). Holding capacity: design method are generally reliable and mature, being similar to those developed for driven piles. Slight uncertainties relate to setup effects in certain soils (as for piles).	Installation: similar to suction caissons, but with a stronger focus on caisson retrieval. Holding capacity: design methods are straightforward for a given plate geometry assuming embedment depth and soil strength are known. Slight uncertainties regarding keying behaviour and response due to cyclic loading.	Installation: relatively mature and less dependent on accurate soil strength profile as higher soil strength which will reduce embedment will be mobilized during loading. Holding capacity: design methods are similar to those developed for driven piles and benefit from a similar reliability level. Uncertainties relate to setup effects (as for piles and caissons) and frameworks for non-vertical loading and cyclic loading are not established.	Installation: similar to torpedo anchors. Holding capacity: comparable to SEPLAs
Design codes	DNV, API and ISO codes - established methods.	Draft ISO code advice, but not prescriptive.	Draft ISO code advice, but not prescriptive.	Falls under SEPLA and torpedo anchor guidance in ISO.

It is useful to examine available performance data for the candidate anchors in order to illustrate their relative performance when upscaled towards the dimensions and capacities required for FLNG applications. Available performance data from various sources are compared in [Figure 3](#). The data are mainly from centrifuge model tests and are expressed in equivalent prototype scale to compare with the Gulf of Mexico unfactored design loads for suction caissons. Evidently the torpedo anchor data offer the lowest capacity, but with a trend that increases essentially linearly with depth reflecting the higher mobilised soil strength at greater depths. However, it is worth noting that although the heaviest torpedo anchor in the centrifuge dataset has comparable weight to the Mad Dog suction caisson (20% less), but the capacity available from the torpedo anchor is much lower. This comparison is influenced somewhat by setup effects, which as reported by [Richardson et al. \(2009\)](#) are significant for torpedo anchors. The torpedo anchor data on [Figure 3](#) typically relates to setup periods of approximately 1 year.

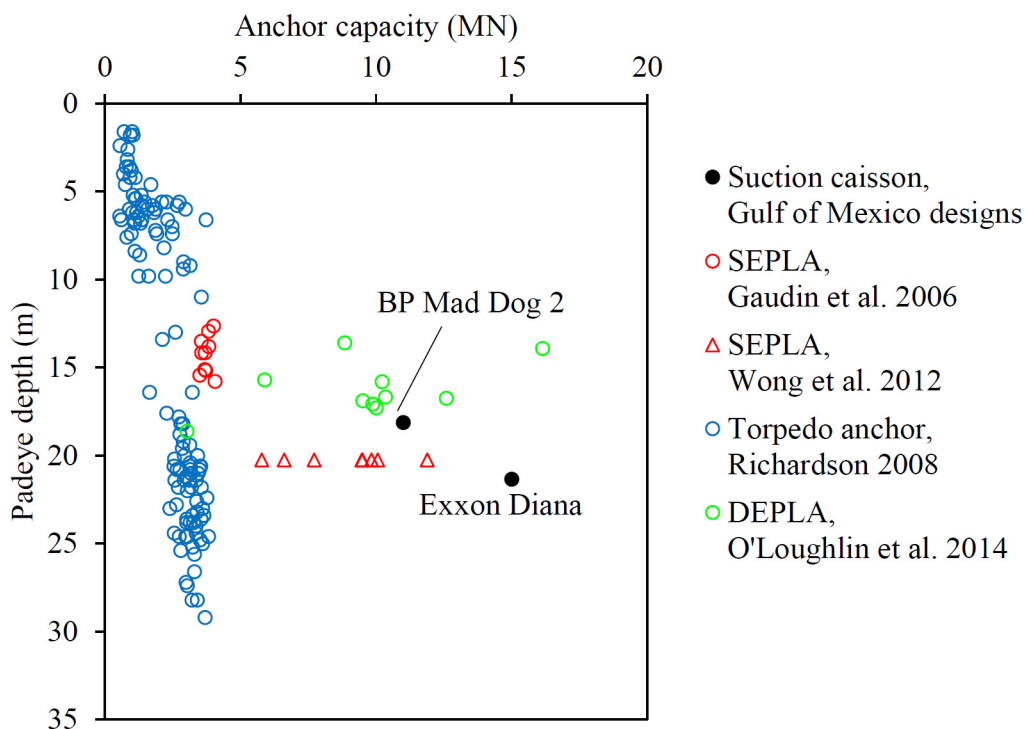


Figure 3—Performance data for each anchor type (data mainly from centrifuge model studies, with suction caisson design examples from Gulf of Mexico).

SEPLA data are reproduced on Figure 3 from centrifuge model studies reported by Gaudin et al. (2006) and Wong et al. (2012). The former utilised a square plate with side length typical of the shorter side of a real rectangular SEPLA. Therefore, the capacity is reduced by up to half compared to a real SEPLA at the same embedment, which typically has a geometrical aspect ratio,  $B/L = 1.5–2$ . The Wong et al. (2012) SEPLA centrifuge data occupy a relatively wide range of capacity, but include two different anchor scales (the larger having 26% higher bearing area) and relate to tests in which various amounts of consolidation were permitted during the keying process. However, the noteworthy aspect of these test data are that they offer capacities that are as high as the Mad Dog suction caisson design load, highlighting the ability of the SEPLA to satisfy high mooring load requirements.

The DEPLA data on Figure 3 are from centrifuge model tests reported by O'Loughlin et al. (2014). The data show a similar range of capacities to the SEPLA, but plot at shallower embedments as the plate is higher on the follower. The scatter in this case is due to significant geometrical differences in the plate. The DEPLA plate area that could be mobilised as bearing resistance differed by a factor of 3.5 across the range of DEPLA geometries tested. DEPLA capacities exceeded both the Mad Dog and Diana caisson design loads. The highest capacity was achieved using a DEPLA that had a combined (follower plus plate) weight that was similar to the Diana caisson. However, the DEPLA plate, which is the load carrying element, weighed only 58% of the caisson, yet provided slightly higher capacity. These results highlight the potential for the DEPLA to also satisfy high mooring load requirements.

Torpedo anchor and DEPLA data from reduced-scale field tests reported by Blake et al. (2015) and O'Beirne et al. (2015) are shown in Figure 4. Again, capacity is seen to increase with depth as expected for this site which has an undrained shear strength gradient of about 1.5 kPa/m (over the depth range shown in Figure 4). The weight of the torpedo anchor is exactly the same as the weight of the combined DEPLA weight (follower plus plate), and about 4 times the weight of the DEPLA plate. Despite this, the DEPLA provides higher capacity, as it resists load in bearing rather than friction.

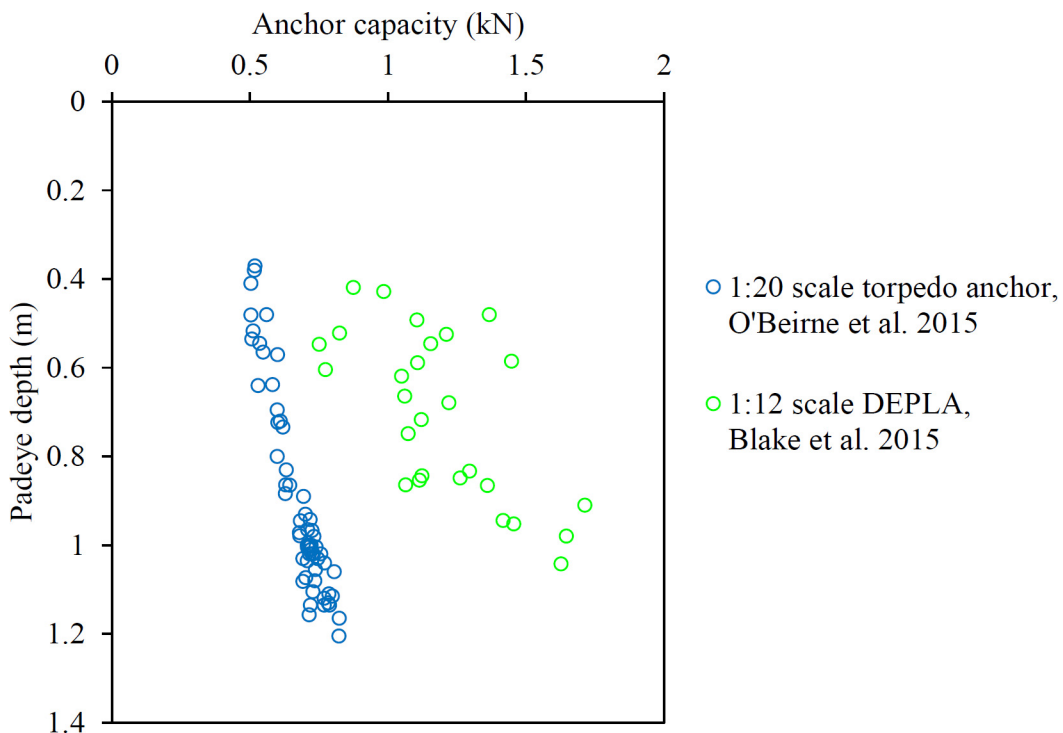


Figure 4—Comparison of model scale field data for torpedo anchor and DEPLA. Note that the mass of the torpedo anchor is the same as the mass of the combined DEPLA follower and plate anchor.

This relative efficiency of the anchors is emphasised by Figure 5 which shows anchor efficiency, defined as the anchor capacity divided by the dry weight. The torpedo anchor and DEPLA data from Figure 4 are shown alongside the larger scale DEPLA data and for the Gulf of Mexico suction caissons referred to earlier. The benefits of the plate anchors are now apparent, with efficiencies approaching 40 compared with < 4 for the torpedo anchor. The suction caisson efficiencies are also relatively low at ~7. This low efficiency is partly because they also resist load partly through friction, when there is a significant component of uplift at the pad-eye, but also because the depth range over which soil resistance is mobilised extends to the surface, where the strength is lower.

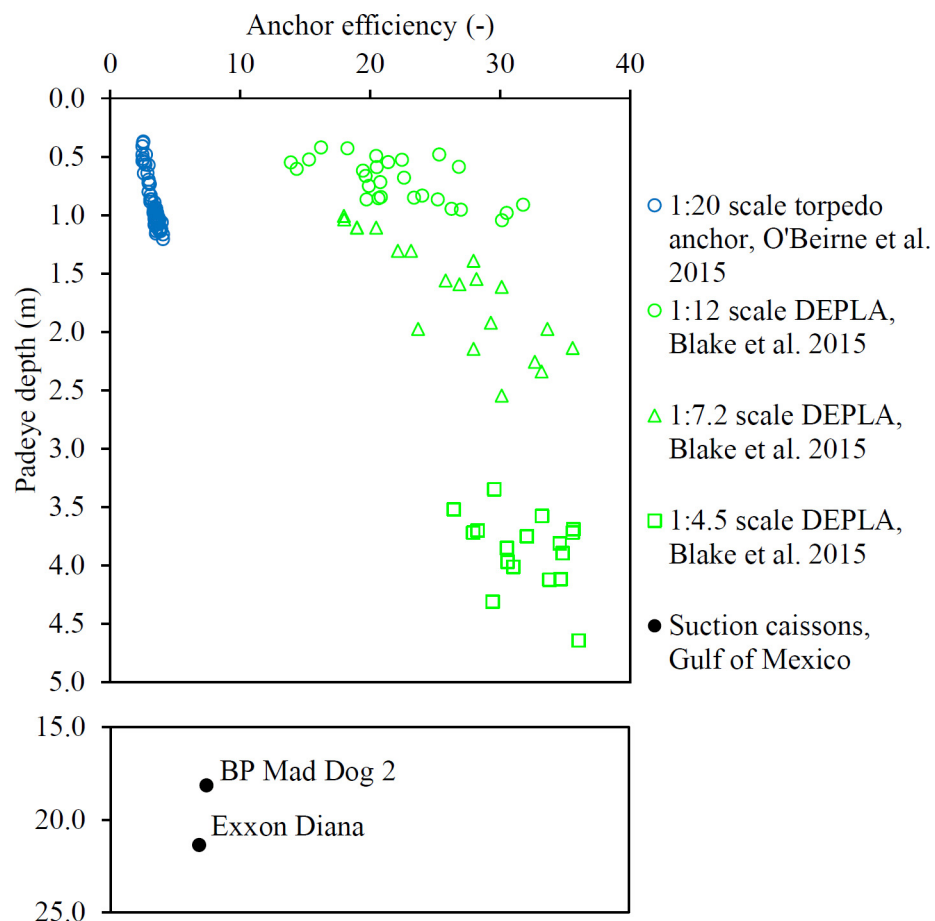


Figure 5—Anchor efficiency: comparison of model scale field data for torpedo anchors and DEPLAs, with suction caisson design data.

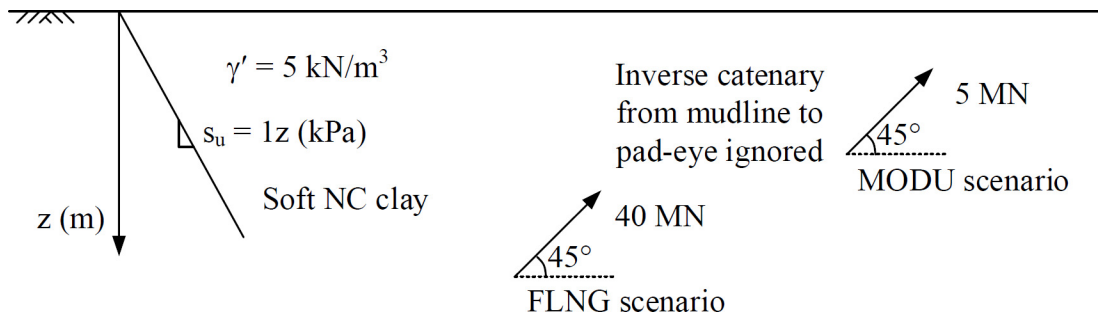
## Concept-level anchor sizing scenario

### Deepwater geotechnical scenario

The anchor sizing analysis has been performed for a simple idealised geotechnical scenario that represents typical deepwater conditions. The soil is normally-consolidated soft clay (or mud) with the properties summarised in Table 2 and shown in Figure 6. The adopted strength gradient is typical for in situ conditions, but includes no reduction for cyclic effects. The interface friction ratio,  $\alpha = \tau/S_u$ , which is the ratio between the shear stress on the wall or shaft of the anchor and the intact soil undrained strength, is relevant for the installation of each anchor type and for the capacity of the suction caisson and the torpedo anchor. A relatively low  $\alpha = 0.3$  was chosen for installation (reflecting a low to medium sensitivity soil), rising to  $\alpha = 0.6$  (due to set-up effects) for capacity mobilization. This factor of two increase is considered broadly appropriate based on published experience with driven piles (Randolph 2003) and suction caissons (Jeanjean 2006)).

**Table 2—Geotechnical properties of design scenario**

Property		Units	Value
In situ (intact) undrained strength, $S_u$ (profile)	Mudline strength, $S_{um}$	kPa	0
	Strength gradient, $ksu$	kPa/m	1
Interface friction ratio, $\alpha$ (for shaft resistance on caisson and torpedo anchor)	Installation	-	0.3
	Capacity	-	0.6
Submerged unit weight, $\gamma'$		kN/m <sup>3</sup>	5

**Figure 6—Specific anchor sizing scenarios.**

### Deepwater FLNG mooring load scenario

These concept-level anchor sizing calculations are simplified and neglect many aspects that would need to be considered in a real anchor design, including: (i) load and resistance partial factors, (ii) cyclic degradation of soil strength, and (iii) tilt and misalignment of the anchor and line. To select representative mooring loads for our sizing calculations, these effects have been accounted for by factoring up a typical design line load.

To determine a suitable level of factoring, the sizing calculations for our base case anchor type - the suction caisson - were first compared to published case studies of anchor dimensions, loads and soil conditions for two of the largest existing applications: Exxon's Diana spar and BP's Mad Dog 2 spar (clusters 1 and 2), both in the Gulf of Mexico. These facilities are both anchored in normally-consolidated clay (Schroeder et al. 2006). The overall safety factor required by ISO 19907-1 (2005) for axial loading of suction anchors in permanent moorings is 2.0. By adopting this factor our simplified calculations yielded a caisson length within 1 m of the actual length adopted in practice, indicating that no other adjustment is required, at least for a concept-level sizing analysis. The adopted load for our FLNG anchor sizing is therefore twice the unfactored line load.

The mooring line load for a large-scale FLNG facility in a deep water location has been estimated as 20 MN per line at an inclination of 45 degrees upwards from the horizontal at the anchor pad-eye. Although this inclination will depend on the mooring line mudline angle and the pad-eye depth, the assumption of a constant 45 degrees is adopted for simplicity. Applying the factor of 2.0 gives a representative load of 40 MN (Figure 6).

The shape and load-carrying effect of the embedded inverse catenary of the mooring line is ignored in this analysis. In practice, the inverse catenary will reduce the load applied at the padeye relative to the at-seabed mooring line load, but will also raise the inclination of that load towards the vertical. The former effect is beneficial since it represents a contribution to the capacity of the anchoring system. The latter effect is negative since anchors have lower capacity at steeper loading inclination. This and other effects associated with the embedded mooring line are discussed later in the paper.

### Deepwater MODU/FPSO mooring load scenario

A representative mooring load for a MODU or FPSO in a deep water location has been selected as 5 MN per line at an inclination of 45 degrees upwards from the horizontal (Figure 6). This value was verified

by comparison with published sizes of MODU suction caissons in the Gulf of Mexico (Jeanjean 2006). Our simple sizing calculations for a suction caisson, using a typical Gulf of Mexico normally-consolidated strength profile, gave anchor dimensions that match those used in practice. As for the FLNG scenario, the chain inverse catenary is ignored.

## Concept-level anchor sizing analysis: methods and assumptions

The calculation methods used in the sizing analysis are summarised in [Table 3](#). The following assumptions were made in the analysis:

**Table 3—Summary of anchor sizing analysis methods**

Anchor	Suction caisson	SEPLA	Torpedo pile	DEPLA
Installation assessment	Check against plug heave ( <a href="#">Randolph &amp; Gourvenec 2011</a> )		Dynamic penetration from impact velocity ( <a href="#">O'Loughlin et al. 2013</a> )	
Capacity assessment	Analytical failure envelopes ( $N_c = 9$ ) ( <a href="#">Randolph &amp; Gourvenec 2011</a> ; <a href="#">Supercharawote et al. 2004</a> )	Keying embedment loss ( <a href="#">Gaudin et al. 2010</a> ) Bearing capacity ( $N_c = 14$ ) ( <a href="#">Wang et al. 2010</a> )	Shaft and tip/tail resistance ( $N_{c,tip} = 12$ , $N_{c,tail} = 9$ , $N_{c,flukes}^{c,flukes} = 7.5$ ) ( <a href="#">O'Loughlin et al. 2004</a> ; <a href="#">O'Beirne et al. 2015</a> )	Keying embedment loss ( <a href="#">Gaudin et al. 2010</a> ; <a href="#">O'Loughlin et al. 2014</a> ) Bearing capacity ( $N_c = 15$ ) ( <a href="#">Wang and O'Loughlin 2014</a> )

- *Suction caisson*: The padeye was assumed to be located at the optimum elevation, such that the line of action of the load passes through the caisson centreline at a depth equal to ~70% of the total caisson length. The bearing and friction factors given in [Table 2](#) were applied, using the calculation methods referenced in [Table 3](#). A sealed top cap was assumed. Typical wall thicknesses based on published case studies were adopted, with the top cap having twice the thickness of the walls.
- *SEPLA*: The dimension ratios of the plate anchor (e.g. L/B, B/t and e/B of the plate, and the L/D ratio of the installation caisson) were based on published SEPLA applications (e.g. [Brown et al. 2010](#)), and scaled to achieve the required capacity. Also, the suction caisson used for installation was checked against plug heave. The weight of the plate was factored by 1.5 to account for the shank to give the overall anchor weight, based on published SEPLA examples.
- *Torpedo anchor*: The dynamic installation was from a height above seabed equal to six times the anchor length, which is typical for published applications for these shapes of anchor. The installation resistance was calculated by combining inertial drag resistance and strain rate-dependent soil strength. The strain rate dependency was modelled using a power law, with an average increase in soil strength of 15% per log cycle increase in strain rate, relative to a reference strain rate of  $0.25 \text{ s}^{-1}$ , which is typical of the average strain rate associated with conventional in situ penetrometer tests. The assumed bulk density of the torpedo pile is based on published examples (e.g. [Lieng et al. 2010](#)). Torpedo piles are typically filled with scrap materials including steel and concrete.
- *DEPLA*: The dynamic installation was from a height equal to six times the anchor length, the same as the torpedo anchor, and the same soil resistance rate effect was considered. The adopted bulk density of the follower assumes it is fabricated from solid steel. This is based on the design of the 1/4 scale trial DEPLA described by [O'Loughlin et al. \(2013\)](#).

This level of analysis is sufficient to provide a realistic comparison between the different anchor types, but is simplified relative to the full geotechnical design of an anchor, in which additional considerations may alter the calculated anchor scales.

## Concept-level anchor sizing results for FLNG and MODU/FPSO scenarios

### Comparison of anchors sizes

The results of the anchor sizing analysis are detailed in [Table 4](#) (FLNG scenario) and [Table 5](#) (MODU/FPSO scenario). The relative sizes and installed depths for the FLNG scenario are indicated in [Figure 7](#), which is shown to scale.

**Table 4—Anchor sizing results: FLNG scenario**

Anchor	Suction caisson	SEPLA	Torpedo anchor	DEPLA
Anchor dimensions	$L = 37.5 \text{ m}$ $d = 7.5 \text{ m}$ $t = 50 \text{ mm}$	$L = 10.8 \text{ m}$ $B = 5.4 \text{ m}$ $e/B = 0.5$ $t = 160 \text{ mm}$	$L = 28.0 \text{ m}$ $d = 2.2 \text{ m}$ $w = 3.4 \text{ m}$ $h = 13.8 \text{ m}$ $t = 129 \text{ mm}$	$D = 7.7 \text{ m}$ $t = 143 \text{ mm}$
Average density in air	$7850 \text{ kN/m}^3$	$7850 \text{ kN/m}^3$ (anchor & follower)	$6259 \text{ kN/m}^3$	$7850 \text{ kN/m}^3$ (anchor & follower)
Follower dimensions	N/A	$L = 48.5 \text{ m}$ $d = 8.1 \text{ m}$	N/A	$L = 19.2 \text{ m}$ $d = 1.5 \text{ m}$
Installed embedment	$37.5 \text{ m}$ (tip)	$48.5 \text{ m}$ (padeye)	$90.4 \text{ m}$ (tip)	$56.2 \text{ m}$ (padeye)
Keyed embedment	N/A	$48.3 \text{ m}$ (padeye)	N/A	$56.0 \text{ m}$ (padeye)
Anchor dry weight	455 tonnes 4.5 MN	109 tonnes 1.1 MN	794 tonnes 7.8 MN	156 tonnes 1.5 MN
Anchor efficiency (capacity/dry weight)	9.0	37.4	4.4	26.1
Installation tool dry weight	N/A	690 tonnes 6.8 MN	N/A	274 tonnes 2.7 MN

**Table 5—Anchor sizing results: MODU/FPSO scenario**

Anchor	Suction caisson	SEPLA	Torpedo anchor	DEPLA
Anchor dimensions	$L = 18.2 \text{ m}$ $d = 3.5 \text{ m}$ $t = 50 \text{ mm}$	$L = 5.4 \text{ m}$ $B = 2.7 \text{ m}$ $e/B = 0.5$ $t = 93 \text{ mm}$	$L = 13.9 \text{ m}$ $d = 1.1 \text{ m}$ $w = 1.7 \text{ m}$ $h = 6.8 \text{ m}$ $t = 64 \text{ mm}$	$D = 3.9 \text{ m}$ $t = 84 \text{ mm}$
Average density in air	$7850 \text{ kN/m}^3$	$7850 \text{ kN/m}^3$ (anchor & follower)	$6259 \text{ kN/m}^3$	$7850 \text{ kN/m}^3$ (anchor & follower)
Follower dimensions	N/A	$L = 24.3 \text{ m}$ $d = 4.1 \text{ m}$	N/A	$L = 9.7 \text{ m}$ $d = 0.8 \text{ m}$
Installed embedment	22 m (tip)	24.3 m (padeye)	45.5 m (tip)	27.5 m (padeye)
Keyed embedment	N/A	24.1 m (padeye)	N/A	27.3 m (padeye)
Anchor dry weight	94 tonnes 0.9 MN	16 tonnes 0.2 MN	98 tonnes 1.0 MN	21 tonnes 0.2 MN
Anchor efficiency (capacity/dry weight)	5.4	32.2	4.4	24.0
Installation tool dry weight	N/A	87 tonnes 0.9 MN	N/A	36 tonnes 0.4 MN

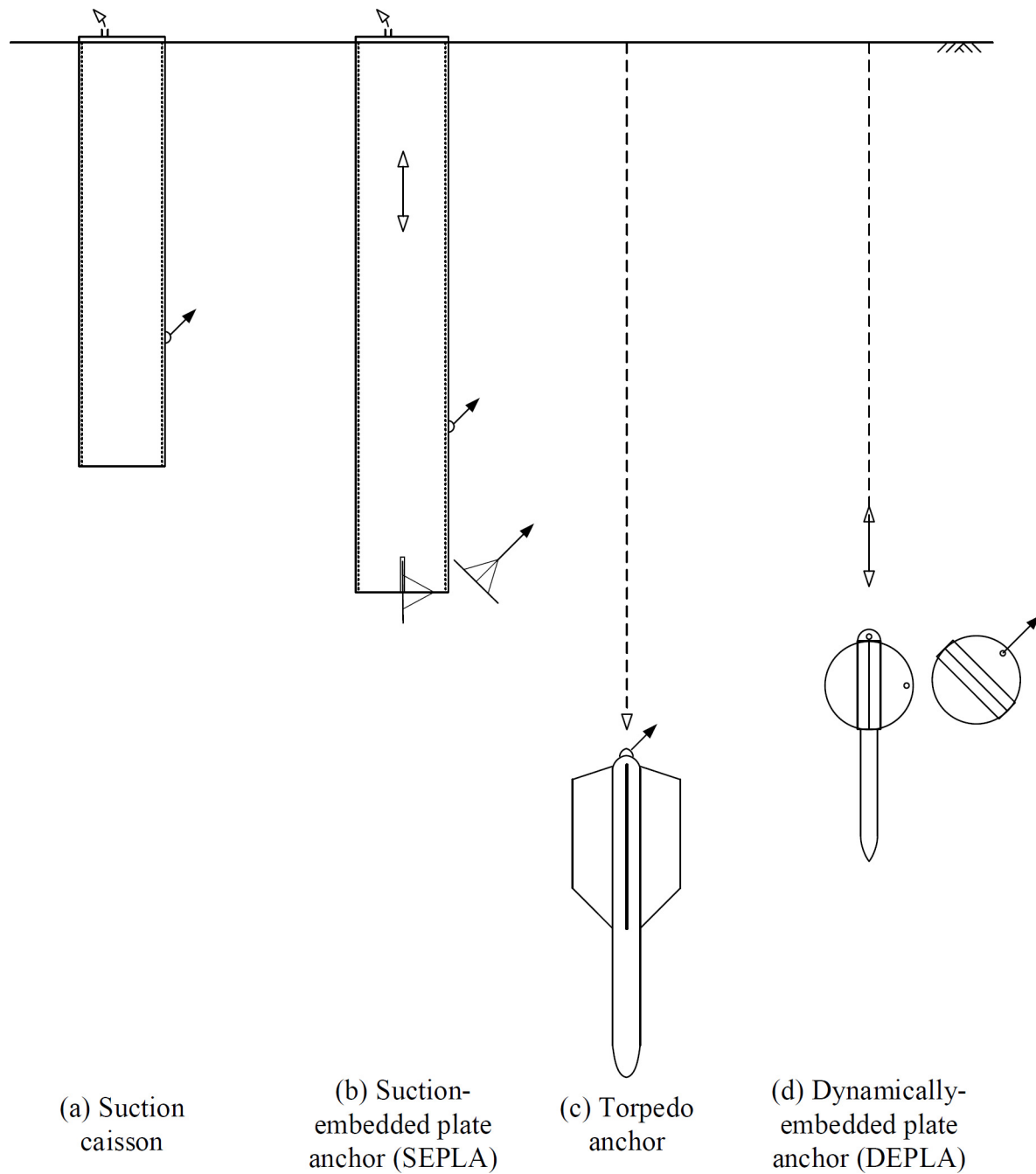


Figure 7—Relative anchor scales and embedment depths from the FLNG concept sizing analysis.

In all cases, the FLNG anchors are larger than previous applications, although the diameter of the suction caisson option matches previous riser tower anchors (which have a shallower penetration depth). The dimensions of the SEPLA and torpedo anchors are beyond existing project cases. The DEPLA flukes are approximately the same size as the SEPLA plates. The DEPLA follower is no larger than existing torpedo anchors used for MODUs (e.g. Aguiar et al. 2011). For the MODU/FPSO scenario, the calculated suction caisson, torpedo and SEPLA sizes match existing practice. The DEPLA follower is smaller than the SEPLA follower.

### Comparison of anchor weights

The weights of the individual anchors and followers are also provided in Table 4 and Table 5, and compared in Figure 8a. The total dry weight of the anchors (and follower if used) for a 12-anchor cluster

is compared in Figure 8b and in Table 6, which also shows the percentage variation in total anchor spread weight relative to the suction caisson (which is considered the ‘base case’).

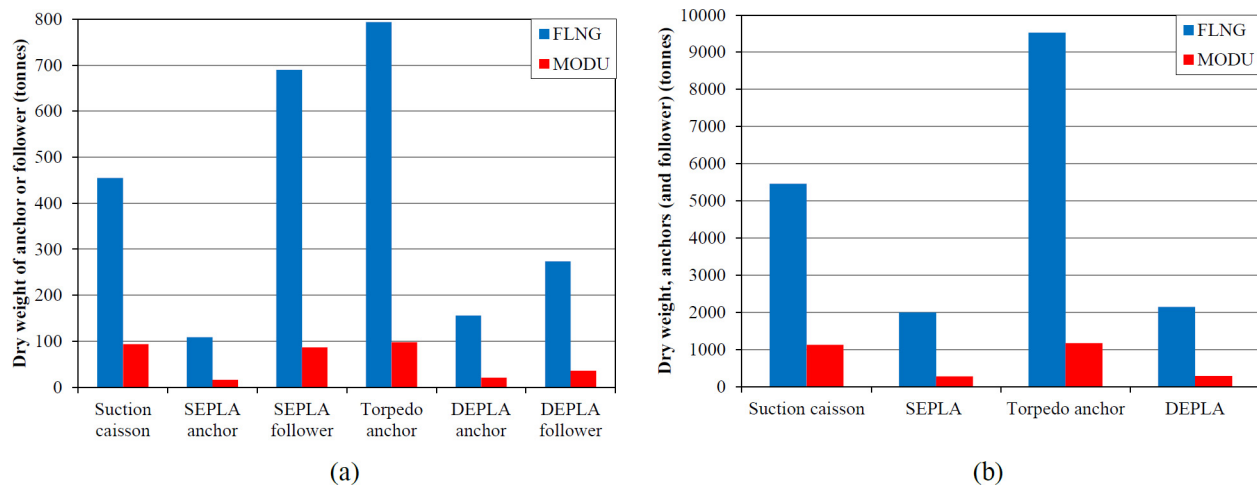


Figure 8—Comparison of anchor and follower dry weights: (a) individual anchors and (b) 12-anchor cluster (and followers if used).

Table 6—Comparison of total dry weight for a 12-anchor cluster

Scenario	Total dry weight of 12 anchors (and follower) (tonnes) (% indicates value relative to suction caisson case)			
	Suction caisson	SEPLA	Torpedo anchor	DEPLA
FLNG	5460 (100%)	2000 (30%)	9530 (175%)	2146 (39%)
FPSO / MODU	1130 (100%)	280 (25%)	1176 (104%)	288 (26%)

For the FLNG scenario, the heaviest individual anchor element is the torpedo anchor, which is almost seven times heavier than any existing torpedo anchor and 75% heavier than the suction caisson. The suction caisson used as a follower for the SEPLA is 52% heavier than that used as an anchor. The DEPLA follower is significantly lighter: it weighs only 35% of the torpedo anchor weight and 40% and 60% of the caisson weight for the suction caisson (anchor) and SEPLA follower respectively. The DEPLA and SEPLA anchors are only 24-34% of the weight of the suction caisson.

For the MODU/FLNG scenario, the calculated weights of the suction caisson, SEPLA and torpedo anchors match existing practice. The SEPLA follower is comparable in weight to the caisson and torpedo anchors, whereas the DEPLA follower is approximately 40% of the weight of the SEPLA caisson follower. The SEPLA and DEPLA anchors are 12-22% of the weight of the suction caisson.

This latter comparison (as for the FLNG scenario) does not consider the weight of the follower as it is reused. This additional weight can be better considered by calculating the weight of a complete spread of anchors, where one follower is required to install each anchor. When combined for a 12-anchor mooring spread, the reduced weight of the SEPLA and DEPLA anchors and the requirement for only a single follower leads to a significant overall reduction in the combined weight of anchors and follower (Figure 8b and Table 6). The SEPLA and DEPLA cases are typically 25% of the overall dry weight of the suction caisson solution for the MODU/FPSO scenario and 30-39% for the FLNG scenario. In contrast, the overall weight of the full spread of torpedo anchors is similar to the suction caissons for the MODU/FPSO scenario, and 75% heavier for the FLNG scenario.

## Fabrication and installation considerations

This section compares the fabrication and installation methods of the different anchor options, and in particular the vessel deck space, crane and time requirements.

## Deck space requirements

The deck space requirement of each anchor option has been estimated on the basis that:

1. A 12-anchor spread is required, plus a follower for the DEPLA and SEPLA options.
2. The anchors and followers are laid down on deck with a 2 m gap between items. Suction caissons, torpedo anchors and followers are laid horizontally. The plate anchors rest flat and the DEPLA anchors stand with the axis vertical (which is the most stable orientation). These arrangements are typical for previous projects (except for the DEPLA, which has not yet been deployed in practice).

This approach is considered sufficient for this comparative analysis, but is likely to underestimate the required deck area since it does not include ancillary equipment. The deck space requirements are compared in [Figure 9](#) and [Table 7](#).

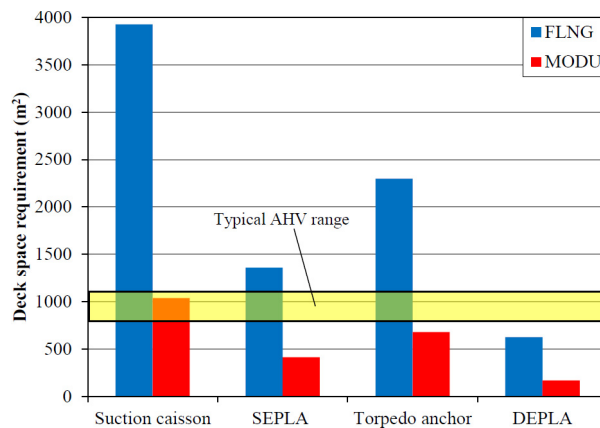


**Figure 9—Deck space requirements for transportation and installation.**

**Table 7—Comparison of deck space requirements for a 12-anchor cluster**

Scenario	Deck space requirement (m <sup>2</sup> ) (% indicates value relative to suction caisson case)			
	Suction caisson	SEPLA	Torpedo anchor	DEPLA
FLNG	3930 (100%)	1360 (35%)	2300 (58%)	620 (16%)
FPSO / MODU	1040 (100%)	410 (40%)	680 (66%)	170 (16%)

The suction caisson option requires by far the most deck space. Compared to the suction caisson, the SEPLA and torpedo anchors require 35-58% and 40-66% of the deck space for the FLNG and MODU/FPSO scenarios respectively, whilst the DEPLA requires only 15% in either case.

Also shown on [Figure 9](#) is an indication of the typical deck space of a large anchor handling vessel (AHV), which ranges from 800–1100 m<sup>2</sup>. All options for MODU/FPSO anchoring can fit on the deck of a single anchor handling vessel. However, this is likely to be due to the deck space required for ancillary items being overlooked in the case of the suction caisson options. When MODUs are anchored by suction caissons, it is common for only half of the spread to be carried on a single AHV.

For the other anchor types, the required deck space for MODU/FPSO anchoring is calculated as around half of the typical AHV deck space. This is consistent with the track record of SEPLA usage for MODUs, in which all anchors can be carried on, and installed from, a single AHV.

The FLNG SEPLA and DEPLA options can potentially fit within the deck space of an AHV (depending on the ancillary equipment required). This is in contrast to the FLNG suction caisson options which require a construction barge for laydown.

## Lifting and winching requirements

The lifting and winching requirements of the vessel for each anchor option have been estimated on the basis that:

1. Crane capacity is required to lift each item (anchor or follower) except that:
2. The SEPLA and DEPLA followers do not need to be lifted, only winched overboard with an anchor attached.

The resulting lifting and winching requirements are summarised in [Figure 10](#). For simplicity, the winching forces are estimated as equal to the dry weight of each item, with no factoring or other allowances.

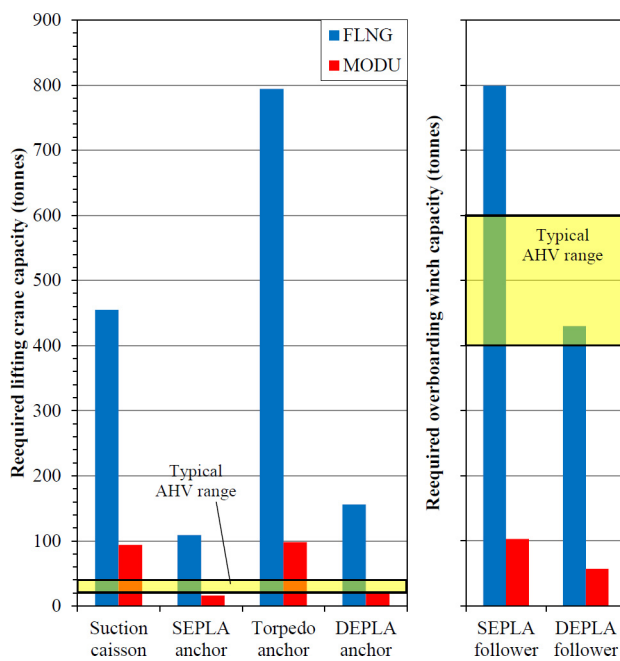


**Figure 10—Lifting and winching requirements for installation.**

AHVs typically have high winch capacities and smaller crane lifting capacities. Typical ranges are indicated in [Figure 10](#). The MODU/FPSO options using SEPLA and DEPLA anchors are within the capacity of typical AHV cranes and winches. In the case of suction caissons and torpedo anchors for MODUs, [Figure 10](#) indicates a greater crane lifting requirement than is usual on an AHV. However, in practice, the requirement for crane lifting is often removed by the use of deck-mounted sliders to position the anchors before overboarding.

The FLNG options using SEPLA and DEPLA anchors are within the capacity of typical AHV winches. However, to manipulate the anchors on deck would require a larger than usual crane or on-deck sliders as currently used for MODU/FPSO suction caissons (which have comparable dry weight).

## Vessel requirements

The deck space and lifting requirements set out above can be combined to indicate the minimum vessel capabilities required for each anchor option. These results are shown in [Table 9](#), but should be considered indicative due to the assumptions outlined previously in the paper. This simple analysis shows that there are clear potential benefits associated with the novel SEPLA, DEPLA and (for the MODU/FPSO case) torpedo anchors. An AHV is far less costly than a construction barge and is more readily mobilised. It is

also more likely to be available independent of other construction work, so there are reduced constraints on scheduling and less knock-on effects to other project operations.

**Table 8—Comparison of lifting crane and overboarding winch requirements**

Scenario	Lifting crane requirement (tonnes)				Overboarding winch requirement (tonnes)	
	Suction caisson	SEPLA	Torpedo anchor	DEPLA	SEPLA	DEPLA
FLNG	455	109	794	156	800	430
FPSO / MODU	94	16	98	21	103	57

**Table 9—Comparison of indicative vessel type and duration requirements for a 12-anchor cluster**

Scenario	Indicative vessel requirement			
	Suction caisson	SEPLA	Torpedo anchor	DEPLA
FLNG	Construction barge (15 days)	AHV <sup>1</sup> (18 days)	Construction barge (6 days)	AHV (9 days)
FPSO / MODU	AHV (2 swings) (14 days)	AHV (15 days)	AHV (5 days)	AHV (7 days)

<sup>1</sup>Although Figure 9 indicates that the SEPLA FLNG option fits a typical AHV deck, this calculation is optimistic because deck space for ancillary equipment is overlooked.

## Installation schedule

The time required for installation of a 12-anchor spread has been estimated using the tentative durations per anchor for each option given in Table 10. These estimates do not include transportation to and from the project location, except for the case of the MODU/FPSO suction caisson installation, which includes an additional 2 days to allow for the AHV only carrying a half-load of anchors. In practice, the installation duration will depend on a wide range of other factors that are either unaffected by the anchor type or which are either unknown at the design stage or are influenced by other project construction activities. This comparison is therefore highly tentative. The total durations for installation of a 12-anchor spread have been calculated from Table 10 and are shown under the indicative vessel type in Table 9. The DEPLA and torpedo anchors offer the most rapid installation.

**Table 10—Estimated durations per anchor installation**

Scenario	Suction caisson	SEPLA	Torpedo anchor	DEPLA
FLNG	1.25 days	1.5 days	0.5 days	0.75 days
FPSO / MODU	1 day	1.25 days	0.4 days	0.6 days

## Cost comparison

The cost of an anchoring system comprises the costs of manufacture and installation (as well as ongoing integrity management costs). No attempt has been made to estimate the cost of the installation, which depends primarily on the vessel type and the time periods of mobilisation, transportation and operations. Vessel day rates vary significantly between regions, and time periods for transportation depend on project location. The choice of vessel may also influenced by the needs of other project activities, particularly if a construction barge is involved. Given these considerations, it is not sensible to attempt a generic comparison. However, it should be possible for project-specific first order estimates to be made based on the anchor sizes set out in the paper and the installation summary information given in Table 9.

The only cost quantifications that have been attempted are the fabrication of the anchors, based simply on the indicative costs of fabricated steel given in [Table 11](#). These costs are likely to be somewhat lower than the cost of purchasing fabricated anchors directly from an anchor supplier, where a commercial mark-up applies to cover other costs. The calculated are therefore only *indicative* and may not be relevant to a particular project situation.

**Table 11—Basis for estimating fabrication costs**

Steel type	Plates	Rolled or cast	Rolled + scrap
Anchor element	Anchor plates and flukes	Followers, caissons	Torpedo anchor
Cost per tonne	\$2,500	\$3,500	\$2,000

The relative fabrication costs essentially mirror the overall weight of each anchor spread, with minor adjustments due to the relative costs for different materials given in [Table 11](#). For the FLNG scenario, the SEPLA and DEPLA anchors offer a potential saving relative to the suction caisson base case of \$13.5M on fabrication costs. As indicated in [Table 9](#), there are likely to be further significant benefits related to vessel type and installation duration. For the MODU/FLNG scenario, the torpedo anchor offers a \$1.5M fabrication cost benefit relative to the suction caisson option, increasing to ~\$3M for the SEPLA and DEPLA. As with the FLNG scenario, there are also installation duration benefits as set out in [Table 9](#).

Despite the approximate and indicative nature of these cost comparisons, they show that the fabrication costs of the novel anchors are significantly smaller than the conventional suction caisson solution.

## Anchor chain considerations

### Influence of anchor chain

The anchor concepts described in this study all feature padeyes located below mudline, to which the mooring line - made from chain - is attached. The concept sizing exercise described above adopted a uniform load and load angle at the padeye for simplicity. In reality, soil resistance acting on the chain will contribute to the overall capacity of the anchoring system, and the inclination of the load at the pad-eye will generally differ from the angle of the mooring line at the mudline due to the shape of the chain within the seabed. This shape forms an inverse catenary, controlled by the weight of the chain and the mobilised soil resistance parallel and normal to the chain.

For catenary moorings, where the chain lies on the seabed for some length between the suspended section and the anchor, the chain direction rotates through the inverse catenary from horizontal to the angle at the pad-eye. This inclination may be vertical if the pad-eye is particularly deep or the soil is strong. This uplift component can be onerous for suction caisson anchor capacity but for the fully embedded plates it often has minimal influence. For taut and semi-taut moorings the angular deviation of the chain through the soil may be minimal, and the pad-eye angle can be within a couple of degrees of the chain angle at mudline.

Solutions for the shape of the chain are based on equilibrium between the chain self-weight, its tension and the soil resistances. This analysis is an extension of the ‘capstan’ equations and allows the chain shape and also the increase in chain tension with distance from the anchor point to be evaluated. The integration of these equations from the anchor point to mudline is often performed numerically, which allows arbitrary profiles of soil strength and resistance to be adopted ([Vivatrat et al. 1982](#), [Degenkamp & Dutta 1989](#)). Analytical expressions that neglect the chain self-weight exist ([Neubecker & Randolph 1995](#)) and these closely approximate the exact solutions without the cumbersome iteration needed with the numerical approach.

The inverse catenary is created when the mooring line is first loaded, pulling the line through the soil. The catenary changes shape as the line load is increased either in-service or during pre-service loading, releasing ‘slack’ into the suspended mooring line. In design, it is necessary to assess the inverse catenary shape under different loads to determine the release of chain slack under the design loads.

### **Requirement for proof loading or pre-loading**

The plate anchors described in this paper have similarities with drag-embedded anchors, which were developed prior to the SEPLA and DEPLA. As a result, design approaches have been borrowed from this prior experience, although not all aspects are necessarily transferable. For example, anchors may require proof loading or test loading for one or more reasons ([ISO 2013](#)):

1. to ensure adequate holding capacity of the anchoring system,
2. to eliminate slack in the embedded portion of the mooring lines, and
3. to allow detection of any significant installation-induced damage to mooring components, with various levels of tensioning required in each case.

Reason (1) is applicable to drag-embedded anchors because it is the proof loading itself that creates the embedment and therefore the capacity of the anchor. This is not the case for the SEPLA and DEPLA and there is no blanket requirement in the current draft ISO 19901/4 and ISO 19901/7 codes for plate anchors and dynamically-installed anchors to be proof loaded to the design holding capacity. For example, for dynamically-installed anchors ISO 19901/4 states that: “*test loading of gravity-embedded [i.e. dynamically-penetrated] anchors to the loading conditions defined in Clause 10.4.6 of ISO 19901–7 [i.e. 80 – 100% of the design load] should not be required as long as the installation records confirm that the minimum required embedment used to calculate the anchor holding capacity is achieved.*”

For plate anchors, it is stated that: “*Plate anchors should be subjected to adequate keying/triggering loading to ensure that sufficient anchor fluke rotation takes place and that the associated loss of penetration depth is within that expected and accounted for in the specification of the target penetration depth.*”

The requirement to proof load anchors to the design load has sometimes been raised as a barrier to the application of SEPLAs, torpedo anchors and DEPLAs for large and permanent moorings. However, historically this requirement to proof load evolved principally from the need to establish and verify the capacity of drag-embedded anchors during installation, and the codes retain a requirement that these anchors shall be proof loaded to 80–100% of the design load.

In contrast, the positional uncertainty on a SEPLA is minimal (it is comparable to a suction anchor), and so predictions of capacity are more reliable. Also, the installed embedment of torpedo anchors and DEPLAs can be determined from monitoring of the freefall and penetration process via a recoverable instrumentation unit (e.g. [Lieng et al. 2010](#)). Having eliminated the positional uncertainty, the remaining uncertainty relates to the soil conditions and the design method adopted – which is no different for a SEPLA or DEPLA compared to a suction anchor or a conventional pile. Consequently there should be no requirement to proof load a SEPLA or DEPLA to the design load (reason 1 above) and this is reflected in the current code requirements. There is therefore no requirement to mobilise an excessively high bollard pull in order to upscale the anchors to MODU/FPSO or FLNG applications. There may remain, however, a need to apply pre-loading to the mooring line after installation to eliminate excessive chain slack in the inverse catenary (depending on the capability of the floating facility to tolerate the slack or correct it) and potentially to provide sufficient keying (reason 2 above).

### **Chain slack assessment**

A set of chain inverse catenary analyses are now presented to examine the additional mooring capacity created by the embedded chain and to explore the potential ‘chain slack’ for the novel SEPLA and DEPLA anchors relative to the conventional suction caisson option. These analyses adopted the same soil strength

profile as the sizing exercise described above, and the chain and chain-soil interaction parameters outlined in [Table 13](#).

**Table 12—*Indicative* fabrication costs for 12-anchor cluster**

<i>Indicative</i> cost (US\$M) for 12-anchor cluster (% indicates value relative to suction caisson case)				
Scenario	Suction caisson	SEPLA	Torpedo anchor	DEPLA
FLNG	19.1	5.7 (30%)	19.1 (100%)	5.6 (30%)
FPSO / MODU	3.9	0.79 (20%)	2.4 (60%)	0.76 (19%)

**Table 13a—Input parameters for embedded chain analyses**

Chain parameters	Value(s)
MODU/FPSO case	Chain bar diameter
	Chain self-weight
	Preload levels
FLNG case	Chain bar diameter
	Chain self-weight
	Preload levels

**Table 13b—Input parameters for embedded chain analyses**

Chain-soil interaction parameters*	Value
Bearing capacity factor for soil resistance normal to chain, $N_c$	9
Equivalent width parameter for soil resistance normal to chain	2.5
Equivalent circumference parameter for soil resistance parallel to chain	8

\* Degenkamp & Dutta (1989), Neubecker & Randolph (1995)

The analyses consider a catenary mooring with a preload applied after installation, horizontally at mudline, 100 m away from the anchor. Two values of pad-eye depth are used, corresponding to the suction caisson and plate anchor (SEPLA and DEPLA) cases set out in [Table 4](#) and [Table 5](#). The results for the MODU/FPSO case are shown in [Figure 12](#) and the FLNG case in [Figure 13](#). To illustrate the chain slack created during in-service loading, an arbitrary location  $x = 500$  m away from the anchor is selected as the limit of the anchoring system. The shape of the inverse catenary to this point is shown in [Figure 12a](#) and [Figure 13a](#), and the chain movement ('slack') and chain load at this location is shown in [Figure 12b](#) and [Figure 13b](#). In addition, the chain tension at the pad-eye is also shown on [Figure 12b](#) and [Figure 13b](#) to illustrate the proportion of the overall load that is carried by the chain in the range  $x < 500$  m.

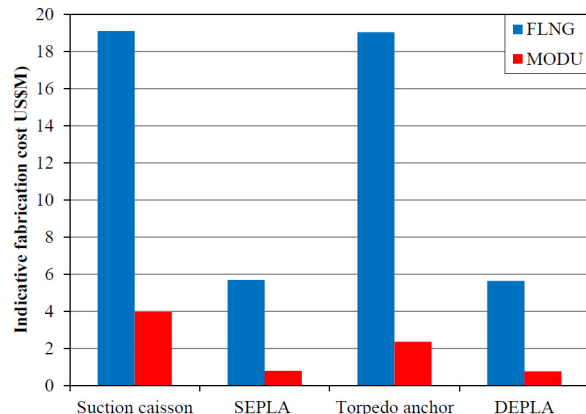
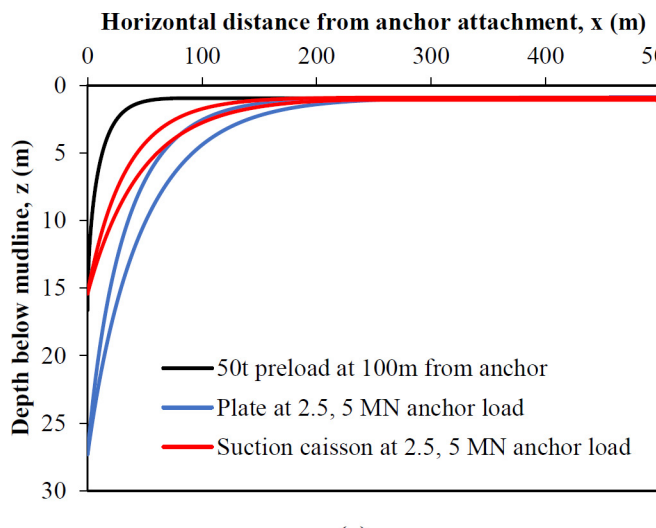
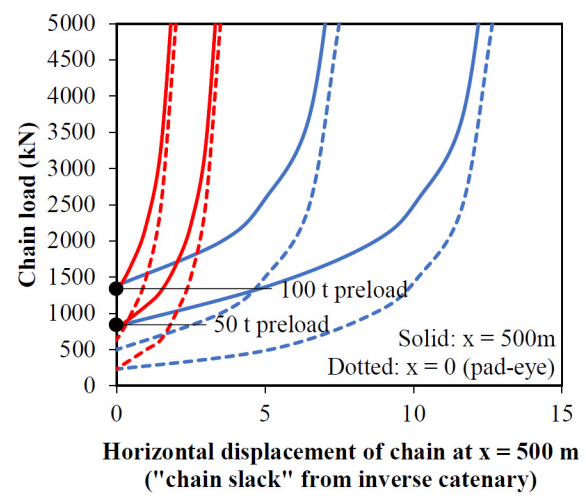


Figure 11—Indicative fabrication cost of 12-anchor spread (and follower if used).



(a)



(b)

Figure 12—Inverse catenary behavior for MODU/FPSO example — suction caisson vs. DEPLA anchor: (a) shape of inverse catenary and (b) “chain slack” generated by loading.

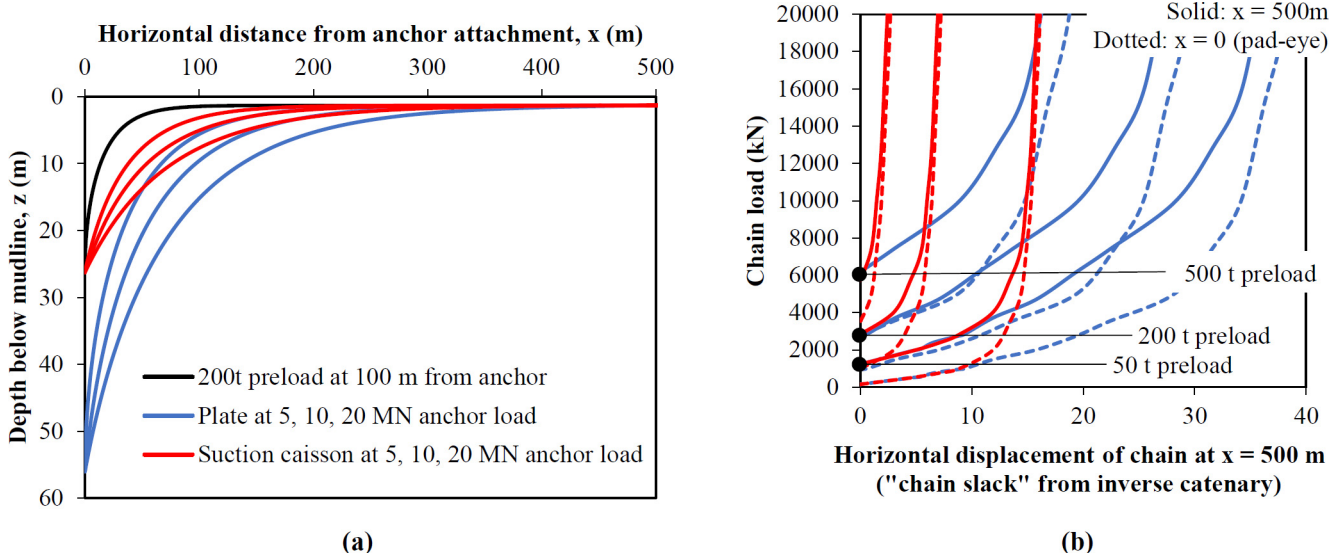


Figure 13—Inverse catenary behavior for FLNG example — suction caisson vs. DEPLA anchor: (a) shape of inverse catenary and (b) “chain slack” generated by loading.

The deeper pad-eye of the plate anchor options leads to greater chain slack, but also a more significant load contribution from the chain. For the MODU/FPSO example, which uses parameters that are typical of real SEPLA applications, a chain slack of 7–12 m is created at the design load of 5 MN compared to < 3 m for the suction caisson cases. In practice, this higher level of chain slack associated with the plate anchors may be tolerated by the mooring system, depending on the mooring dynamics and the capacity to re-tension the mooring lines in service.

The load contribution from the chain represents an additional 1-1.5 MN of mooring load for the plate anchors in the MODU/FPSO example (Figure 12b), which is double the chain load for the shallower suction caisson option. Given that this chain load represents 30% of the design load, the plate anchors could be shallower and/or smaller but still provide adequate capacity. This would in turn reduce the level of chain slack. To reach the optimum choice of anchor system requires iteration considering the composite response of the anchor and chain.

The FLNG example (Figure 13) provides similar observations. The comparison of 3 different preload levels shows the value of maximising the preload that is applied, to minimize the chain slack mobilised in service. For the suction caisson option, the 500 t preload case eliminates ~12 m of chain slack, leaving only 2 m at the 20 MN design load. Such high preloads are costly to apply due to the vessel requirements, but this is balanced against the system stiffness required by the mooring dynamics. For the plate anchor option, the chain slack is higher, and 12 m of slack is mobilized at 20 MN even after 500 t of preload. Again, the embedded chain carries a significant proportion of the total load (typically 50%) for the plate anchor option, compared to 10–20% for the suction caisson case.

When the additional load carried by the embedded chain in a catenary mooring is considered, the sizing analysis described earlier in the paper is biased towards shallower anchors because a uniform pad-eye load is assumed. In practice, the deep SEPLA and DEPLA options can be slightly smaller and shallower. This will lead to a reduced, but potentially still onerous, level of chain slack. For taut and semi-taut moorings that feature an inclined chain at mudline, the chain slack (and the contribution of chain capacity) is far lower than the examples in Figure 12 and Figure 13.

The results of this chain response analysis are based on adoption of previously-reported values for the chain-soil interaction parameters (Degenkamp & Dutta 1989). These parameters for the embedded chain were originally calibrated from model tests involving monotonic tensioning of chain inverse catenaries (e.g. Vivatrat et al 1982). Given the recent discoveries of complex chain-seabed interaction effects

including massive trenching and erosion (Bhattacharjee et al. 2014), as well as complex remoulding, consolidation and trenching behaviour around steel catenary riser touchdown zones (Bridge & Howells 2007, Hodder et al. 2009), it is timely to revisit these assumptions - as discussed in the following section.

### **Chain-seabed interaction behaviour: physical modelling observations**

The chain-soil interaction parameters given in Table 13 lead to embedded chain-soil resistance, using notation in Figure 15, of:

1. Normal resistance (stress) of  $N_c S_u$  acting on an effective width of  $2.5D_{bar}$ , where  $N_c = 9$ , corresponding to flow around a cylinder and  $S_u$  is taken as the initial soil strength.
2. Parallel resistance of  $S_u$  acting on a circumference of  $8D_{bar}$  (implying a cylinder of effective diameter  $\sim 2.5D_{bar}$ ).

The equivalent friction (i.e. parallel/normal resistance) for embedded chain is therefore 0.36. However, for on-bottom chain an equivalent friction coefficient of 0.7–1.0 is typically recommended in design (e.g. ISO 2005). This creates an inconsistency in the solution of the inverse catenary - which approaches the seabed asymptotically for normally-consolidated conditions - because it implies a step increase in parallel resistance acting on the chain at the location where the inverse catenary is defined as ending, with chain reverting from ‘embedded’ to ‘on-bottom’.

Meanwhile, the recent observations of trenching and soil erosion around mooring lines and in riser touchdown zones suggest that cyclic movement of a chain or riser leads to remoulding and softening of the seabed soil. This would imply a reduction in both the normal and parallel resistance on the embedded chain, as the operative value of  $S_u$  is reduced.

A recent centrifuge modelling pilot study was performed at the University of Western Australia to quantify the friction and burial behaviour of on-bottom anchor chain. The tests were performed in a range of soils but only results from soft kaolin clay are presented here. The apparatus comprised a length of model chain supported at each end and pulled horizontally over the soil bed (Figure 14). A potentiometer mounted at the mid-point of the chain was used to track the vertical settlement. This signal was used to control the vertical movement of the arms holding the ends of the chain, to ensure that the applied loading acted horizontally. Axial load cells at each end of the model chain measured the applied horizontal force per unit length,  $T$ . The chain dimensions and self-weight are given in Table 14, following the notation shown in Figure 15.

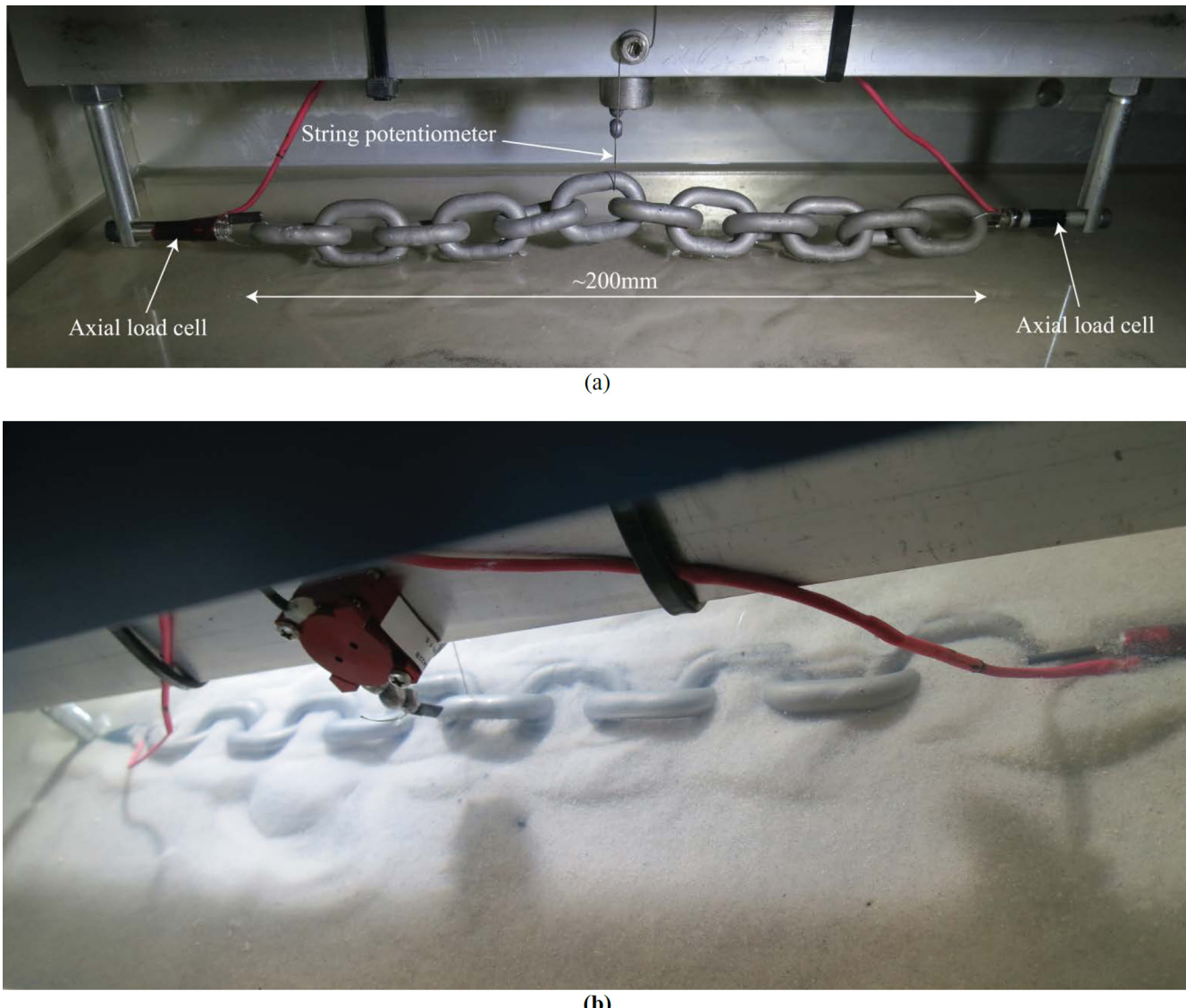


Figure 14—Centrifuge modelling arrangement for chain-seabed interaction testing.

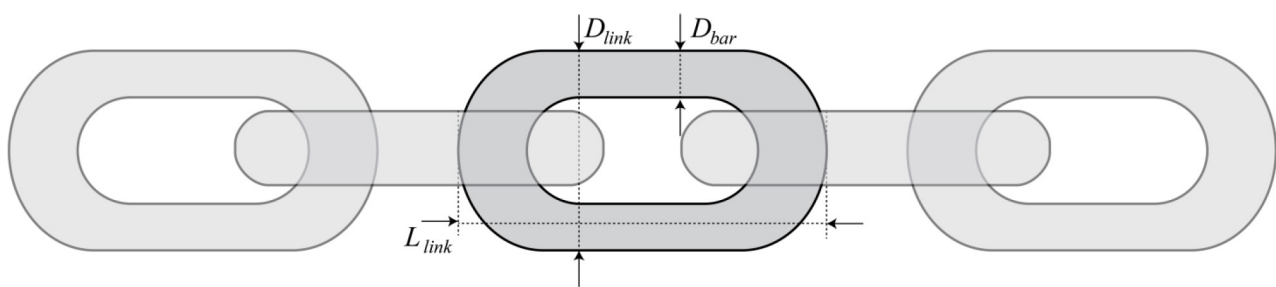
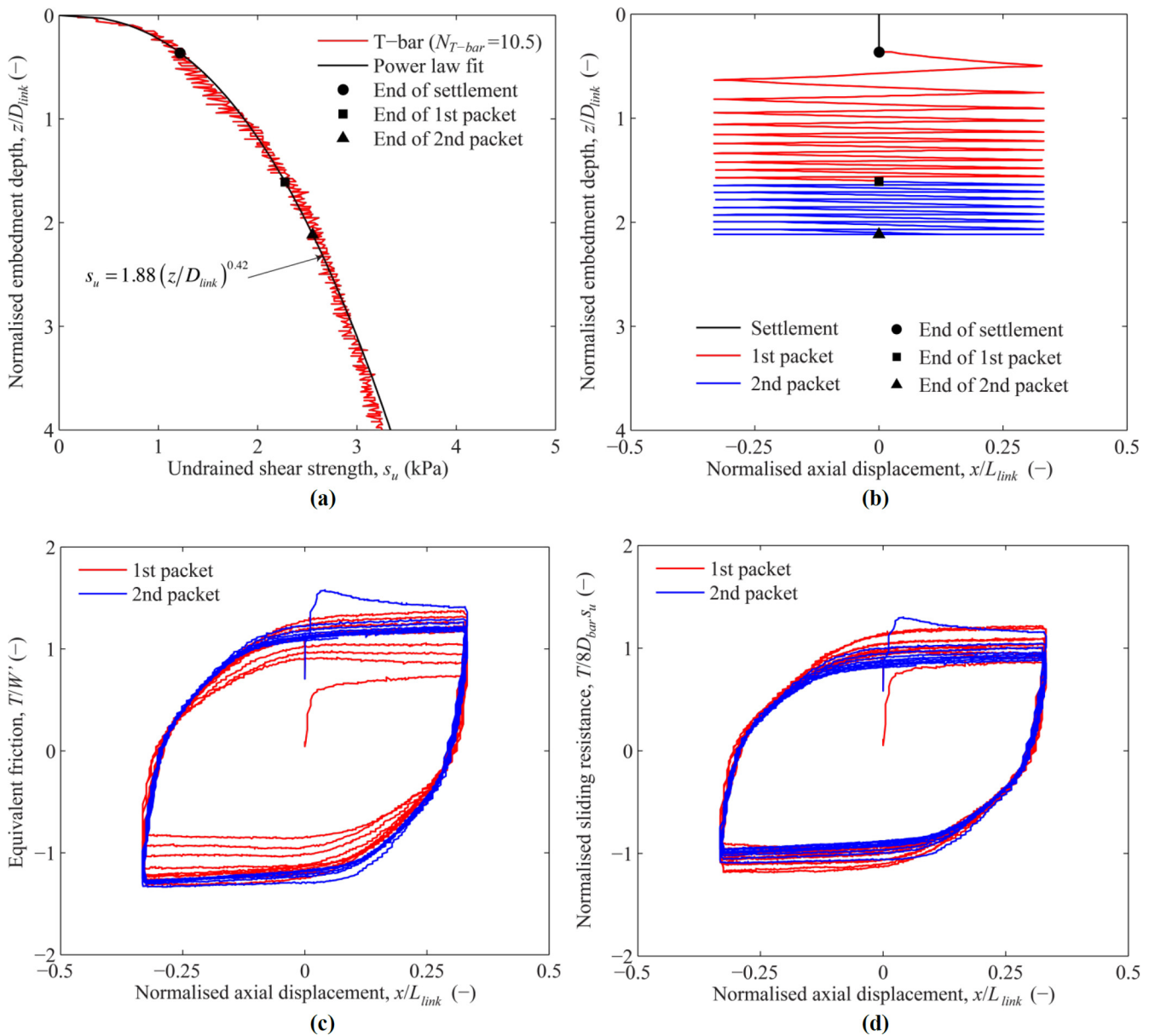


Figure 15—Notation for chain dimensions.

**Table 14—Parameters of model chain tests**

Chain parameters	Value	
	Model	Prototype (at 15 g)
Dimensions		
Bar diameter, $D_{\text{bar}}$	6 mm	90 mm
Link width, $D_{\text{link}}$	21.5 mm	322.5 mm
Link length, $L_{\text{link}}$	30 mm	450 mm
Self-weight per unit length, $W'$	100 N/m	1500 N/m
Nominal bearing pressure, $q_{\text{chain}} = W'/(2.5D_{\text{bar}})$	6.7 kPa	

The bed of kaolin clay was prepared by self-weight consolidation in-flight at a centrifuge acceleration of 45 g. The sample was then slowed to an acceleration of 15 g and allowed to swell to equilibrium before testing commenced. T-bar tests were performed to determine the undrained strength characteristics. A penetration profile converted to the initial undrained strength,  $s_u$ , is shown in [Figure 16a](#). Cycles of T-bar penetration indicated a sensitivity (initial/remoulded T-bar strength) of ~2.5.



**Figure 16—Measurements of chain on-bottom sliding resistance and sinkage:** (a) soil strength profile, (b) chain sinkage during laying and two packets of axial cycles, (c) equivalent friction response during axial cycles and (d) normalised sliding resistance based on cylindrical failure.

For the example test presented here, the chain penetrated to an embedment of  $z/D_{link} \sim 0.4$  when lowered under self-weight, where  $z$  is the mid-depth of the chain. This corresponds to a bearing ratio of  $q_{chain}/S_u \sim 6.7$  kPa / 1.2 kPa  $\sim 5$ , which is consistent with bearing capacity theory.

The chain was then subjected to two packets of 10 cycles of axial movement of amplitude  $\pm 0.3 D_{link}$ , mobilising parallel resistance,  $T$ . These cycles caused sinkage of the chain significantly below the mudline with soil flowing back over the top of the chain. A consolidation period of 9 days (at prototype scale) was permitted between each packet of cycles.

The equivalent friction,  $T/W'$  rose from  $\sim 0.8$  during the initial forward movement to a steady value of  $\sim 1.3$  during the initial 10 cycles. This level of equivalent friction was sustained through the second packet of cycles after the consolidation period.

The chain settled throughout the cycles at a diminishing rate. The continuing settlement indicates some level of soil remoulding, leading to local weakening that causes additional settlement. The axial resistance

has been normalised consistent with the chain-soil interaction parameters given in Table 13, as  $T/(8D_{\text{bar}})S_u$  so a value of unity implies the initial shear strength  $S_u$  acting on a cylinder of diameter 2.5  $D_{\text{bar}}$ . The normalised resistance is close to this value after some softening in the first few cycles of each packet. The prediction is remarkably accurate, albeit through compensating effects: the operative strength is likely to be less than  $S_u$ , but the effective area of shearing per unit length must be greater than  $8D_{\text{bar}}$ .

However, the sinkage of the chain is significantly underpredicted using the parameters in Table 13. The chain embedment is  $z/D_{\text{link}} \sim 2$  where the initial strength is  $S_u \sim 2.5$  kPa. This yields a bearing ratio of  $q_{\text{chain}}/S_u = 2.7$  on the effective width of 2.5  $D_{\text{bar}}$ . This value is lower than the theoretical  $N_c = 9$ , which can be attributed to (i) the effect of combined axial and lateral loading (which reduces  $N_c$  by  $2/3$  in the presence of axial sliding, Aubeny et al. 2003) and (ii) remoulding of the surrounding soil, based on the T-bar sensitivity of 2.5. These modifications suggest a bearing ratio of 2.4, which is very close to the observed value.

In summary, from this limited dataset, it appears that the chain embedment after cycles of movement tends to a limit linked to the remoulded soil strength and a bearing factor associated the combined axial-vertical loading. The corresponding axial resistance is consistent with shearing at the intact soil strength on a cylinder of diameter 2.5  $D_{\text{bar}}$ , albeit probably due to compensating errors in the assumptions. It is expected that the behaviour would be the same if the chain had been dragged monotonically in one direction, because of the complex shearing that accompanies soil flow over and through the chain links. The results are therefore expected to apply when the chain is loaded monotonically in service, such as during the development of chain slack modelled earlier in this paper, which involves chain movements of several link lengths.

These results, if confirmed through further investigation, have implications for conventional chain modelling including the analyses presented earlier. They suggest that higher equivalent friction values are appropriate for modelling the inverse catenary, leading to additional capacity from the chain. Also, the additional chain sinkage will lead to flatter catenaries with reduced chain slack effects and reduced uplift loading at the anchor.

## **Summary: Anchor technology opportunities**

The anchor sizing exercise shows potentially significant cost benefits associated with SEPLA and DEPLA anchors for both MODU/FPSO and FLNG applications. Torpedo anchors also offer benefits in the MODU/FPSO scenario, which have already been exploited in practice. However, offset against these benefits is the relative immaturity of these novel anchor technologies - particularly the DEPLA - relative to the suction caisson base case.

The analysis and physical modelling of chain-seabed interaction described above also highlight potential benefits from improved modelling of this behaviour, both via an increased contribution to the anchor system capacity and less onerous chain slack and pad-eye loading directions.

The key uncertainties and opportunities identified in this study are listed in Table 15. The torpedo anchor is not considered given the poor performance in the cost/weight comparisons when upscaled to the FLNG application.

**Table 15—Design and performance uncertainties and opportunities**

Design consideration	Anchor type		
	Suction caisson	SEPLA	DEPLA
Long term effects	N/A	Potential benefit from set-up and consolidation vs. degradation from cyclic loading.	
Soil type		Performance in carbonate soils (for Australian and other applications)	
Geotechnical reliability	N/A	N/A	Potential improved reliability (or lower FoS) due to capacity being weakly dependent on soil strength (strength variations are compensated by change in dynamic embedment). Verify dynamic embedment step outs: carbonate soils, scale/strain rate effect
Proof loading and/or keying	N/A	Benefit from clarifying/reducing requirements for proof loading and/or keying.	
Chain-seabed interaction		Reconcile inconsistencies between modelling of embedded and on-bottom chain. Address apparent under-estimation of chain friction and self-burial in current practice.	
Mooring system interaction		Clarify tolerance of mooring system to chain slack derived from (i) pullout of the inverse catenary and (ii) keying of plate anchors, during preloading and in operation	
Installation misalignment and keying strategy	N/A	Potential for misalignment and keying strategy to be determined.	
Structural capacity	N/A		N/A

In summary (by rows in Table 15):

- The long term performance of SEPLA and DEPLA anchors under cyclic loading is not well understood. There is evidence from recent research that the long term performance may be significantly better than currently assumed because the beneficial effect of consolidation may outweigh the degradation from cyclic loading.
- The performance of all the anchors in carbonate soils such as found in deep water frontiers offshore Australia is uncertain relative to other soil conditions. Existing design methods generally require further validation for these soils.
- Dynamically-installed anchors such as the DEPLA are less susceptible to soil strength uncertainty, because their installed depth is self-corrected for soil strength variations. This effect can be quantified within a reliability framework, and could remove over-conservatism and allow reduced partial factors relative to other anchors.
- A requirement for plate anchors to be proof-loaded to their design load is sometimes raised as a barrier that prevents their adoption for large permanent moorings, due to the low bollard pull available from installation vessels. However, a common basis for requiring anchors to be proof-loaded has been the uncertain embedment reached by drag-embedded anchors. This does not apply to the SEPLA and is less applicable to the DEPLA as current instrumentation technology allows the embedment to be monitored during installation. The current draft ISO code for anchors has no blanket requirement for SEPLAs and DEPLAs to be proof-loaded to the design load. It is important to clarify this logic amongst design practitioners such that an appropriate requirement can be agreed in projects.
- It appears that the chain component of the anchoring system may be modelled over-conservatively, based on a pilot study reported in this paper. The results suggest that there is potentially additional capacity available from the embedded chain, as well as a less onerous loading angle at the pad-eye. Improved modelling may also resolve inconsistencies between the current design advice for

embedded and on-bottom chain. Improved modelling of chain-seabed interaction deserves urgent attention, in light of recent field observations of mooring line trenching causing reduced anchoring system capacity.

- The interaction between the anchor, chain and mooring line puts certain constraints on the anchor design. In particular, the level of chain slack calculated for deeply-embedded plates in this study may not be consistent with limits assumed in the mooring analysis. It may be possible to tolerate more relaxed limits on chain slack, which will unlock the potential cost benefits of the novel anchors, without adverse impact on the mooring system dynamics.
- Finally, it is also important to quantify the misalignment potential of the novel DEPLA and SEPLA anchors during installation and keying from out-of-plane loading, which has not been the focus of research to date.

## Summary and conclusions

This paper has explored the impact of the upscaling of anchoring loads created by large FLNG vessels on the most appropriate anchor technology, as well as reviewing emerging anchor technologies for more general MODU and FPSO applications.

The study has identified opportunities for significant cost and schedule savings for the anchoring of FLNG facilities as well as MODU/FPSOs, by adopting the alternative plate anchor technologies of SEPLAs and DEPLAs. Based on *fabrication costs alone*, the *indicative* estimated saving is \$13.5M for FLNG and \$3M for MODUs relative to the conventional suction caisson option. When installation vessel costs are considered, the FLNG saving could be far higher, because installation could be from an anchor-handling vessel rather than a construction barge with a heavy lift crane. Torpedo anchors have also been considered, but are much less attractive for FLNG applications, whilst remaining a viable alternative for MODU and FPSO applications.

Analyses presented in the paper that predict the inverse catenary of the embedded mooring line, demonstrate that the embedded chain carries a significant proportion of the total load. For FLNG applications this is typically 50% for the plate anchor option, compared to 10-20% for the suction caisson case. This presents an added benefit as it allows the SEPLA and DEPLA options to be slightly smaller and shallower. However, this will lead to a reduced, but potentially still onerous, level of chain slack that will be released into the mooring. An opportunity arises if the current limitations on mooring line slack can be relaxed or if slack that does occur can be remediated whilst in-service. Physical model testing also shows that the current assumptions used in chain-soil modelling may underestimate the frictional resistance and lead to an overly-conservative shape of inverse catenary.

In summary, there are potential opportunities to unlock more cost effective anchoring for both FLNG and MODU/FPSO applications through a combination of research and qualification activities. Research is required to provide better guidance on the load-carrying capability of mooring lines, both on and within the seabed. Related to this are activities that should address the true tolerance of mooring systems to chain slack, as relaxing this requirement will limit the required pre-loading required for hook-up. At the same time campaigns are required to deploy plate anchors - particularly the new DEPLA - at larger scales such that qualifications can be sought. Regardless of whether conventional suction caissons or novel plate anchors are preferred, future FLNG facilities will require a step-out in anchoring capacity, with a significant impact from the assumed chain-seabed interaction. Some of the future planned projects are in challenging soils such as Australia's deepwater carbonate muds, and the range of anchoring technologies and research advances described in this paper will contribute to the reduction in cost and risk.

## Acknowledgements

This work forms part of the activities of the Centre for Offshore Foundation Systems (COFS), currently supported as a node of the Australian Research Council Centre of Excellence for Geotechnical Science

and Engineering and as a Centre of Excellence by the Lloyd's Register Foundation. The Lloyd's Register Foundation invests in science, engineering and technology for public benefit, worldwide. The second author acknowledges the support of Shell Australia, through the Shell EMI Chair in Offshore Engineering at UWA.

## References

- Aguiar, C.S., Sousa J.R.M., Ellwanger, G.B., Fernandes, J.V.V. and Henriques, P.R.D. (2011). Numerical simulation of installed torpedo anchors embedded in cohesive soil. *Proceedings of the International Conference on Offshore Mechanics and Arctic Engineering, OMAE2011-49646*.
- Aubeny, C.P., Han, S.W. and Murff, J.D. (2003). Inclined load capacity of suction caissons. *International Journal of Numerical and Analytical Methods in Geomechanics*, **27**, 1235–1254.
- Bhattacharjee, S., Majhi, S.M., Smith, D. and Garrity, R. (2014). Serpentina FPSO Mooring Integrity Issues and System Replacement: Unique Fast Track Approach. *Proceedings of the Offshore Technology Conference*, Houston, Texas, OTC 25449.
- Blake, A.P. and O'Loughlin, C.D. (2012). Field testing of a reduced scale dynamically embedded plate anchor. *Proceedings of the 7th International Conference on Offshore Site Investigation and Geotechnics*, London, UK, 621–628.
- Blake, A.P. and O'Loughlin, C.D. (2015). Installation of dynamically embedded plate anchors as assessed through field tests, *Canadian Geotechnical Journal*, *in press*.
- Blake, A.P., O'Loughlin, C.D. and Gaudin, C. (2015). Capacity of dynamically embedded plate anchors as assessed through field tests, *Canadian Geotechnical Journal*, **52** (1), 87–95, doi: 10.1139/cgj-2013-0473.
- Brandao, F.E.N., Henriques, C.C.D., Araujo, J.B., Ferreira, O.C.G. and Amaral, C.D.S. (2006). Albacora Leste field development - FPSO P- 50 mooring system concept and installation. *Proceedings of the Offshore Technology Conference*, Houston, Texas, OTC 18243.
- Bridge, C., and Howells, H. (2007). Steel catenary riser touchdown point vertical interaction models. *Proceedings of the Offshore Technology Conference*, OTC 16628.
- Brown, R.P., Wong, P.C. and Audibert, J.M. (2010). SEPLA keying prediction method based on full-scale offshore tests. *Proceedings of the 2nd International Symposium on the Frontiers in Offshore Geotechnics*, Perth, Australia, 717–722.
- Cassidy M.J., Gaudin C., Randolph M.F., Wong P.C., Wang D. and Tian Y. (2012). A plasticity model to assess the keying behaviour and performance of plate anchors. *Géotechnique*, **62** (9), 825–836.
- Degenkamp, G. and Dutta, A. (1989). Soil resistances to embedded anchor chain in soft clay. *Journal of Geotechnical Engineering ASCE*, **115** (10), 1420–1438.
- Gaudin, C., O'Loughlin, C.D., Randolph, M.F. and Lowmass, A. (2006). Influence of the installation process on the performance of Suction Embedded Plate Anchors. *Géotechnique*, **56** (6), 389–391.
- Gaudin, C., Simkin, M., White, D.J., O'Loughlin, C.D. (2010). Experimental investigation into the influence of keying flap on the keying plate anchors. *Proceedings of the 20th International Offshore and Polar Engineering Conference (ISOPE)*, California, USA, **2**, 533–540.
- Gaudin, C., O'Loughlin, C.D., Hossain, M.S. and Zimmerman, E. (2013). The performance of dynamically embedded anchors in calcareous silt. *Proceedings of the 32nd International Conference on Ocean, Offshore and Arctic Engineering, OMAE2013-10115*.
- Gaudin, C., Tian, Y., Cassidy, M.J., Randolph, M.F. and O'Loughlin, C.D. (2015). Design and performance of suction embedded plate anchors. *Proceedings of the 3rd International Conference on Frontiers in Offshore Geotechnics*, Oslo, Norway, forthcoming.
- Henriques, P.R.D., Foppa, D., Porto, E.C., and Medeiros, C.J. (2010). A New Torpedo Pile Conception for High Mooring Loads and Application in a Floating Production Unity in the Pre-Salt Area. *Proceedings of the Rio Oil & Gas Expo and Conference 2010, IBP3355\_10*, Rio de Janeiro, Brazil.

- Hodder M., White D.J. and Cassidy M.J. (2009). Effect of remolding and reconsolidation on the touchdown stiffness of a steel catenary riser: observations from centrifuge modelling. *Proc. Offshore Technology Conference*, Houston, USA. Paper OTC19871-PP
- Hossain, M.S., O'Loughlin, C.D. and Kim, Y. (2015). Dynamic installation and monotonic pull-out of a torpedo anchor in calcareous silt, *Géotechnique*, *in press*, doi: 10.1680/geot.13.P.153.
- ISO 19901-7 (2005). Petroleum and natural gas industries - Specific requirements for offshore structures - Part 7: Station keeping systems for floating offshore structures and mobile offshore units. *International Organization for Standardization*, Geneva, Switzerland.
- ISO 19901-4 (2013) [OGP 119901-4]. Petroleum and natural gas industries - Specific requirements for offshore structures - Part 4: Part 4: Geotechnical and foundation design considerations. Draft, November 2013. International Association of Oil and Gas Producers. / *International Organization for Standardization*, Geneva, Switzerland.
- Jeanjean, P. (2006). Setup characteristics of suction anchors for soft Gulf of Mexico clays: Experience from field installation and retrieval. *Proceedings of the Annual Offshore Technology Conference*, Houston, Texas, OTC 18005.
- Lieng, J.T., Tjelta, T.I. and Skaugset, K. (2010). Installation of two prototype deep penetrating anchors at the Gjøa Field in the North Sea. *Proceedings of the 2010 Offshore Technology Conference*, paper OTC 20758.
- Neubecker, S. and Randolph, M.F. (1995). Profile and Frictional Capacity of Embedded Anchor Chains. *Journal of Geotechnical Engineering ASCE*, **121** (11), 797–803.
- Randolph, M.F. (2003). 43rd Rankine Lecture: Science and empiricism in pile foundation design. *Géotechnique*, **53** (10), 847–875.
- Randolph, M.F. and Gourvenec, S.M. (2011). *Offshore Geotechnical Engineering*, Spon Press, New York.
- Richardson, M.D., O'Loughlin, C.D. and Randolph, M.F. (2006). Drum centrifuge modelling of Dynamically Penetrating Anchors. *Proceedings of the 6th International Conference on Physical Modelling in Geotechnics*, **1**, 673–678.
- Richardson, M., O'Loughlin, C.D., Randolph, M.F. and Gaudin, C. (2009). Setup following installation of dynamic anchors in normally consolidated clay. *ASCE Journal of Geotechnical and Geoenvironmental Engineering*, **135** (4), 487–496.
- Song, Z., Hu, Y., O'Loughlin, C.D. and Randolph, M.F. (2009). Loss in anchor embedment during plate anchor keying in clay. *ASCE Journal of Geotechnical and Geoenvironmental Engineering*, **135** (10), 1475–1485.
- O'Beirne, C., O'Loughlin, C.D., Wang, D. and Gaudin, C. (2015). Capacity of dynamically installed anchors as assessed through field testing and three dimensional large deformation finite element analyses. *Canadian Geotechnical Journal*, *in press*, doi: 10.1139/cgj-2014-0209.
- O'Loughlin, C.D., Randolph, M.F. and Richardson, M. (2004). Experimental and theoretical studies of Deep Penetrating Anchors. *Proceedings of the 2004 Offshore Technology Conference*, paper OTC 16841.
- O'Loughlin, C.D., Lowmass, A., Gaudin, C., and Randolph, M.F. (2006). Physical modelling to assess keying characteristics of plate anchors. *Proceedings of the 6th International Conference on Physical Modelling in Geotechnics*, **1**, 659–665.
- O'Loughlin, C.D., Richardson, M.D. and Randolph, M.F. (2009). Centrifuge tests on dynamically installed anchors. *Proceedings of the 28th International Conference on Ocean, Offshore and Arctic Engineering*, OMAE2009–80238.
- O'Loughlin, C.D., Blake, A.P., Wang, D. Gaudin, C., Randolph, M.F. (2013). The Dynamically Embedded Plate Anchor: results from an experimental and numerical study. *Proceedings of the 32nd International Conference on Ocean, Offshore and Arctic Engineering*, OMAE2013–11571.

- O'Loughlin, C.D., Blake, A.P., Richardson, M.D., Randolph, M.F. and Gaudin, C. (2014). Installation and capacity of dynamically embedded plate anchors as assessed through centrifuge tests. *Ocean Engineering*, doi 10.1016/j.oceaneng.2014.06.020.
- O'Loughlin, C.D., Blake, A.P. and Gaudin, C. (2015). Towards a design method for dynamically embedded plate anchors. *Géotechnique, under review*.
- Schroeder, K., Andersen, K.H., and Jeanjean, P. (2006). Predicted and Observed Installation Behavior of the Mad Dog Anchors. *Proceedings of the 2006 Offshore Technology Conference*, Houston, Texas, OTC 17950.
- Shell (2014) *Shell Prelude E-news*, Edition 4, June 2014. <http://www.shell.com.au/aboutshell/who-we-are/shell-au/operations/upstream/prelude/prelude-media-centre/prelude-eneews.html>
- Supachawarote, C., Randolph, M.F. and Gourvenec, S. (2004). Inclined pull-out capacity of suction caissons. *Proceedings of the 14th International Offshore and Polar Engineering Conference (ISOPE)*, California, USA, 2, pp. 500–506.
- Tian Y., Gaudin C. and Cassidy M.J. (2014). Improving plate anchor design with a keying flap. *Journal of Geotechnical and Geoenvironmental Engineering, ASCE*, **140** (5), 04014009.
- Vivatrat, V., Valent, P.J. and Ponterio, A.A. (1982). The influence of chain friction on anchor pile design. *Proceedings of the 14th Offshore Technology Conference*, Society of Petroleum Engineers, Richardson, TX, 153–163.
- Wang, D., Hu, Y. and Randolph, M.F. (2010). Three-dimensional large deformation finite-element analysis of plate anchors in uniform clay. *ASCE Journal of Geotechnical and Geoenvironmental Engineering*, **136** (2), 355–365.
- Wang, D., Hu, Y. and Randolph, M.F. (2011). Keying of rectangular plate anchors in normally consolidated clays. *Journal of Geotechnical and Geoenvironmental Engineering*, **137** (12), 1244–1253.
- Wang, D. and O'Loughlin, C.D. (2014). Numerical study of pull-out capacities of dynamically embedded plate anchors, *Canadian Geotechnical Journal*, doi 10.1139/cgj-2013-0485.
- Wilde, B., Treu, H. and Fulton, T. (2001). Field testing of suction embedded plate anchors. *Proceedings of the 11th International Symposium on Offshore and Polar Engineering (ISOPE)*, Stavanger, 2, 544–551.
- Wong P., Gaudin C., Randolph M. F., Cassidy M. J. and Tian Y. (2012) Performance of suction embedded plate anchors in permanent mooring applications. *Proceedings of the 22nd International Offshore and Polar Engineering Conference*, Greece. 2, 640–645.
- Yang, M., Aubeny, C.P. and Murff, J.D. (2012). Behaviour of suction embedded plate anchors during the keying process. *Journal of Geotechnical and Geoenvironmental Engineering, ASCE*, **138** (2), 174–183.
- Zimmerman, E. H., Smith, M. W. and Shelton, J.T. (2009). Efficient Gravity Installed Anchor for Deepwater Mooring. *Proceedings of the Offshore Technology Conference*, Houston, Texas, oTc 20117.